NOVEL DESIGN OF RF MEMS SWITCH WITH REDUCTION IN STRESS GRADIENT TO INCREASE RELIABILITY

DISSERTATION – II

Submitted in partial fulfillment of the requirement for the award of the Degree of

MASTER OF TECHNOLOGY

IN

Manufacturing Engineering

By

(Abhishek Chauhan)

Under the Guidance of

Mr. Harpreet Singh

(Assistant Professor)

(School of Mechanical and Manufacturing Engineering)

Lovely Professional University

Punjab

MAY, 2015

NOVEL DESIGN OF RF MEMS SWITCH WITH REDUCTION IN STRESS GRADIENT TO INCREASE RELIABILITY

DISSERTATION - II

Submitted in partial fulfillment of the requirement for the award of the Degree of

MASTER OF TECHNOLOGY

IN

Manufacturing Engineering

By

(Abhishek Chauhan)

Under the Guidance of

Mr. Harpreet Singh

(Assistant Professor)

(School of Mechanical and Manufacturing Engineering)

Lovely Professional University

Punjab

Lovely Professional University Jalandhar, Punjab

CERTIFICATE

I hereby certify that the work which is being presented in the dissertation entitled **"NOVEL DESIGN OF RF MEMS SWITCH WITH REDUCTION IN STRESS GRADIENT TO INCREASE RELIABILITY"** in partial fulfillment of the requirement for the award of degree of **Master of Technology (Manufacturing Engineering)** and submitted in Department of Mechanical Engineering, Lovely Professional University, Punjab is an authentic record of my own work carried out during period of Dissertation under the supervision of **Mr. Harpreet Singh**, **Assistant Professor**, Department of Mechanical Engineering, Lovely Professional University, Punjab.

The matter presented in this dissertation has not been submitted by me anywhere for the award of any other degree or to any other institute.

Date:

(Abhishek Chauhan)
Reg. No. 11305393

This is to certify that the above statement made by the candidate is correct to best of my knowledge.

Date: **(Harpreet Singh)**
Supervisor

The M- Tech Dissertation examination of Abhishek Chauhan, has been held on_____

Signature of Examiner

LOVELY PROFESSIONAL UNIVERSITY
PHAGWARA – 144402, PUNJAB

CANDIDATE DECLARATION

I, Abhishek Chauhan, Reg. No. 11305393 hereby declare that the work presented entitled "**NOVEL DESIGN OF RF MEMS SWITCH WITH REDUCTION IN STRESS GRADIENT TO INCREASE RELIABILITY**" in partial fulfillment of requirements for the award of Degree of Master of Technology (Manufacturing Technology) submitted to the Department of Mechanical Engineering at Lovely Professional University, Phagwara is an authentic record of my own work carried out during the period from JAN 2014 to MAY 2015, under the supervision of Mr. Harpreet Singh (Assistant Professor), Department of Mechanical Engineering. The matter presented in this thesis has not been submitted in any other University/ Institute for the award of Degree of Master of Technology. Furthermore, I also declare that I will not publish this work in any other Journals/ Conferences/ Workshop seminars except the one chosen by supervisor. The presented work is the property of Lovely Professional University, Phagwara. If I found violating any of the above conditions, University has right to cancel my degree.

Signature of Student Date:

Place:

ABSTRACT

This paper displays a novel cantilever RF MEMS switch. This paper reports on the design and modelling of a low-actuation voltage Microelectromechanical System (MEMS) switch for high-frequency applications mainly in k-band. The mechanical design of low spring-constant crab leg and serpentine beams is presented first, and then using these beams to demonstrate with measured actuation voltages of as low as 1-6V, also the effective stress and actuation voltage required for cantilever membranes is analyzed using finite element modeling. The thickness (t) 1.4 μm, width (w) 50 μm, length (L) is 360 μm of membrane is used. In the present work, MEMS Cantilever Switches are used due to low power consumption, high sensitivity and IC compatibility long life cycles and free from temperature effects. There are many materials being used to made substrate but in present work used silicon-di-oxide. By using same approach to make cantilever switch, simulation of the design is done on COMSOL MULTIPHYSICS 5.0 software. For the purpose of study, a novel design of membrane which is actuated on COPLANER WAVEGUIDE by using the 0.5 microns thickness of dielectric silicon nitride. Further, the results analysis is determining von Mises stress of membrane and contact force. The computed von Misses stress is 200 $\mu N/m^2$ and total average displacement of membrane determined to be 0.12 μm. Li (2009) used a cantilever design for the cantilever switch in which the stress gradients are found out to be around 5400 $\mu N/m^2$ or 5.4 Gpa while with the application of the hybrid cantilever serpentine and crab leg flexure a drastic change was observed in the stress gradient in which the stress is found out to be 200 $\mu N/m^2$ or 0.02 Gpa. This difference of stress gradients of around 5200 Gpa shows that, the new design of the beam is found out to be very effective and the very designing of the switch is revolutionized. As for the issues of adhesion, Bhushan (2003) presented a very important review regarding causes of stiction and adhesion, along with methods to reduce the stiction and different measurement techniques in commercial and magnetic storage devices.

Keywords: Microelectromechanical systems (MEMS), k-bands, RF Membrane, Stress gradient, Flexures, Reliability

ACKNOWLEDGEMENT

Nothing can be achieved without an optimal combination of inspiration and perspiration. The real spirit of achieving a goal is through the way of excellence and discipline. I would have never succeeded in completing my task without the cooperation, encouragement and help provided to me by various personalities.

I owe my special thanks to Mr. Harpreet Singh, Assistant Professor, Department of Mechanical Engineering, LPU, Jalandhar, who helped and guided me for this work. His encouraging remarks from time to time greatly helped me in improving my skills. I wish to place on record my gratitude for all those who have been instrument in bringing my work to this stage.

I do not find enough words with which I can express my feeling of thanks to all my friends for their help, inspiration and moral support which went a long way in completion of my thesis.

Above all I render my gratitude to the ALMIGHTY who bestowed me self-confidence, ability and strength to complete this work. I also owe thanks to my parents for their support and encouragement.

ABHISHEK CHAUHAN

Reg. No. 11008897

LIST OF FIGURES

LIST OF TABLES

NOMENCLATURE

CPW	Coplanar Waveguide
MEMS	Microelectromechanical System
RF	Radio Frequency
Al	Aluminum
Au	Gold
Cu	Copper
dB	Decibels
GaAr	Gallium Arsenide
GHz	GIGA Hertz
mW	Micro Watt
nH	Nano Hertz
Ni	Nickel
nJ	Nano Joule
Rh	Ruthenium
Ru	Rubidium
V	Voltage
ω	Angular Velocity
Ω	Ohm
$	Dollar
°	Degree
µ	Micro
µm	Micrometer
µs	Micro Seconds
Å	Angstrong

CONTENTS

CHAPTER 1: INTRODUCTION

1.1 RADIO FREQUENCY MICRO ELECTRO MECHANICAL SWITCHES

Small scale Electro Mechanical switches working at radio frequencies have been the subject of scrutinizes for in the course of recent years. Different plans of RF-MEMS switches which are incited through electrostatic, attractive, piezoelectric or thermally actuated powers have been effectively utilized as a part of different satellite and safeguard applications. As portrayed by Lee (2009) the most regularly utilized among these are electrostatically impelled MEMS switch, because of their slightest force utilization, good seclusion, least insertion loss, linearity and low intermodulation items in exchanging operations, Mushtafa (2009) demonstrated that in an electrostatic power is affected between the altered terminal and versatile pillar, which causes the mechanical incitation of the shaft over the RF signal. Explores have prompted two primary sorts of RF-MEMS switches: settled altered bar and cantilever sort. These switches utilize the flexible quality of the pillar structure to restore the moving part to its unique position, when electrostatic powers are evacuated. Consideration has been paid to upgrade these essential plans lately. RF-MEMS switches likewise have couple of issues, which incorporate lacking dependability, high incitation voltage, and low power taking care of capacity and moderately low exchanging paces portrayed by Fonseca (2011). Different endeavors have been made to evacuate staying, and attain to high unwavering quality outlines of MEMS switches as proposed by Kuo (2006).

1.2 PURPOSE OF RF SWITCH

RF MEMS switches offer numerous favorable circumstances over standard strong state switches regarding low loss, high segregation, low power utilization and high linearity. The detriments of MEMS switches are low exchanging rate (μs extent) and high incitation voltage. In numerous telecom utilizations of RF exchanging, these downsides don't give any real issue. A few strategies have been accounted for the outline of high-seclusion switches. MEMS switches are miniaturized scale machined gadgets that utilization mechanical development to have a short out or an open circuit in the RF transmission-line. MEMS RF switches are as metal-to-metal contact switches and capacitive switches. In the metal contact switch, there is direct contact between the transmission line and the shaft. The resistive contact switch licenses operation down to DC. The recurrence of operation acquired for these switches is DC-110 GHz. In the capacitive switches, the contact is by means of a protecting dielectric layer, as inquired about by DeGroot (2009). The blocking

capacitor stops the low recurrence flags going through. The recurrence of operation reported for these switches is 30-120 GHz.

1.3 EVOLUTION OF MEMS

From the year 1990, MEMS rose with the advancement of coordinated circuit (IC) manufacture forms, in which sensors, actuators, and control capacities were created in silicon also proposed by Yoon (2006). From that point forward, amazing exploration advances have been attained to in MEMS under the solid capital speculations from both government and commercial ventures. Notwithstanding the urbanization of some less coordinated MEMS gadgets, for example, miniaturized scale accelerometers, inkjet printer head, small scale mirrors for projection, and so forth., the ideas of more perplexing MEMS gadgets have been proposed and exhibited for the applications in fields as small scale fluidics, aviation, biomedical, concoction investigation, remote correspondences, information stockpiling, showcase, optics, and so on. The greater part of MEMS gadgets with different detecting or activating systems were produced utilizing silicon mass micromachining, surface micromachining, and lithography, Galvano shaping, forming (LIGA) forms as utilized by Passi (2012). Three-dimensional smaller scale manufacture procedures utilizing more materials were formulated for MEMS as of late, when some particular application prerequisites (e.g., biomedical gadgets) and the small scale actuators with higher yield force were required in MEMS. Micromachining is the principal innovation for the manufacture of MEMS Silicon micromachining is the most developed and later of the micromachining advances, and it helps the assembling of MEMS that have measurements in the sub millimeter extent. It alludes to forming tiny mechanical parts out of silicon substrate or on a silicon substrate, making the structures three dimensional and giving new morals to new standards to the originators. Utilizing materials, for example, crystalline silicon, polycrystalline silicon, silicon nitride, and so forth., an unlimited mixture of mechanical microstructures including shafts, stomachs, grooves, openings, springs, apparatuses, suspensions, and an extraordinary differences of other complex mechanical structures have been imagined.

1.4 HISTORY OF RF MEMS

The historical backdrop of MEMS is valuable to delineate its differing qualities, difficulties and applications. The accompanying rundown abridges a percentage of the key MEMS turning points.

1958 Silicon strain gages industrially accessible.

1959 "There's Plenty of Room at the Bottom" – Richard Feynman gives a development presentation at California Institute of Technology. He issues an open test by offering $1000 to the first individual to make an electrical engine littler than 1/64th of an inch.

1961 First silicon weight sensor illustrated.

1967 Invention of surface micromachining, Westinghouse makes the Resonant Gate Field Effect Transistor, (RGT) and Description of utilization of conciliatory material to free micromechanical gadgets from the silicon substrate.

1970 First silicon accelerometer illustrated.

1979 First miniaturized scale machined inkjet spout.

1980 First investigations in surface small scale machined silicon and micromachining influences microelectronics industry and far reaching experimentation and documentation builds open premium.

1982 Make a Disposable pulse transducer.

1982 LIGA Process is hung on creation.

1988 First MEMS meeting arranges.

Routines for micromachining pointed towards enhancing sensors.

1992 MCNC begins the Multi-User MEMS Process (MUMPS) supported by Defense Advanced. Research Projects Agency (DARPA).

1992 First small scale machined pivot.

1993 First surface small scale machined accelerometer sold (Analog Devices, ADXL50).

1994 Deep Reactive Ion Etching is licensed.

1995 Bio-MEMS quickly creates.

2000 MEMS optical-organizing parts get to be huge business.

1.5 BASIC PARAMETERS FOR RF MEMS

Electrical vitality is effectively transported by method for conveyors, for example, wires or transport bars, which can be controlled by transfers or switches. In a straightforward electric circuit, the foremost parts are a wellspring of electrical vitality, a heap or a yield gadget and a

complete way for the flow of current. In the event that any of the above prerequisites is not fulfilled, current can't flow in the circuit and the vitality from the source can't be conveyed to the yield gadget.

Different parameters to be considered in the outline of RF switches are:

I. Transition time.
II. Switching rate.
III. Switching transients.
IV. RF power handling.
V. Matching with circuit.
VI. Bandwidth.
VII. Insertion loss.
VIII. Isolation.
IX. Series resistance.
X. Actuation voltage.
XI. Lifetime.
XII. Resonant frequency.
XIII. Interception and level of distortion.
XIV. Phase and amplitude tracking.

Aside from these, switches taking into account mechanical activation plans have a couple of extra parameters to be considered. Life-cycle and resounding recurrence of the mechanical part are the most imperative of these. The parameters connected with smaller scale electromechanical framework

(i) Transition time

The transition time is a measure of rate with which the position of a switch can be flipped. This is defined as the time needed for the yield RF sign to ascend from 10% to 90% for off-to-on transition and 90% to 10% for on-to-off transition. As such, it is the time taken for the yield voltage to change to inside 1dB of the final state. In a straightforward mechanical switch, the transition time is the time needed for the moving contact to abandon one stationary contact and strike the inverse stationary contact.

(ii) Switching rate

The switching rate additionally speaks to the time for flipping starting with one condition of the switch then onto the next. Be that as it may, for this situation, the time is measured from 50% on the control voltage to 90% of the RF encompass when the switch is turned on. So also, when the switch is killed, the time is measured till the RF signal voltage achieves 10% of the first. Subsequently, the switching rate is the time needed for the change to react at the yield because of the adjustment in control voltage. Different postpones, for example, driver deferral and driver ascent time is added to the mechanical switching time or the move time. Hence, a semiconductor-controlled switch is much speedier than a mechanical one. The switching rate, additionally alluded to as switching rate, is constantly bigger than the move time of a switch.

(iii) Switching transients

Exchanging transients are the exponentially decaying voltage spikes at the data, yield or both of a RF signal way, because of an adjustment in the control voltage. These exchanging transients are regularly called sidebands because of exchanging, and it indicates essential signs of the execution of an exchanging framework as noted by Jau (2009). It is regularly needed to screen the yield RF range amid the configuration of a RF framework, and consequently segments of the RF chain, for example, amplifiers and switches, must be tried with a referred to boost as utilized by Srikar (2003). Both electromechanical and electromagnetic transients exist amid the exchanging methodology. While the electromechanical transient is because of mechanical movement (wherever present) of the switch component, the electromagnetic transient is because of vitality trade between electric fields and attractive fields of the electric gear in the system. It might be noticed that these transients emerge from nonlinearities in the system. The exchanging transients in PIN diode changes are because of the put away charge in the natural area being immediately released by the control voltage in adjusted Schottky hindrance outlines, the charge put away by the diode is little and most of the transients are brought on by the crisscross inside the drive circuits utilized by Zaghloul (2011). On the other hand, the exchanging transient component of the gallium arsenide field impact transistor (GaAs FET) MMIC circuits results when the quickly changing entryway voltage is coupled to the switch yield through the door to channel capacitance of the FET, in this manner encountering a more prominent nourish through in light of its quicker exchanging.

(iv) RF power handling

RF power handling is a measure of how efficiently a switch passes the RF signal. This is generally specified regarding a 1dB pressure point, which is embraced from the amplifier portrayal industry. It is usually expected that the yield power level takes after the data power with a direct proportion. Anyhow, in numerous gadgets there is a most extreme power above which this linearity does not hold. The 1dB pressure point is defined as the most extreme information power level at which the yield power contrasts by 1dB concerning linearity. The 1dB pressure focuses and the power handling of numerous gadgets, for example, PIN diodes and MMIC switches are elements of rec

(v) Impedance matching

Impedance coordinating is a basic component in all high-recurrence plan. The exchanging gadget ought to be coordinated at both info and yield sides, for both the on and the off condition of the change, to minimize its effect on the execution of whatever remains of the framework. A despicably coordinated part brings about undesirable reflections inside the circuit, which can bring about significant harm to different frameworks. Despite the fact that a perfect match is occasional accomplished, consideration ought to be taken to minimize the reflections inside adequate breaking point.

(vi) Available bandwidth

Albeit the majority of the exchanging frameworks don't have a farthest point on the most reduced recurrence of operation, they do have a maximum utmost. For semiconductor gadgets this is because of the finite time in transporter versatility. The misfortunes acquired from resistance and parasitic reactances are the primary driver restricting the execution of electromechanical switches at higher frequencies.

(vii) Insertion loss

The insertion loss of a RF gadget is a measure of its efficiency for sign transmission. On account of a switch, the insertion loss is specified just when its state is such that flag is transmitting or when the switch is on state. This is specified as far as the transmission coefficient, S21, in decibels, between the info and yield terminals of the exchanged circuit. Typically specified in decibels, one of the outline objectives for a large portion of the RF changes is to minimize the insertion loss. The insertion loss has a tendency to debase with increment in recurrence for the vast majority of the strong state exchanging frameworks. Contrasted and these, RF MEMS switches can be intended to work with a little insertion loss at a few gigahertz. Resistive losses at lower frequencies and skin-depth impacts at higher frequencies are the significant foundations.

(viii) Isolation

The isolation of an exchanging framework is specified when there is no sign transmission. This is likewise measured as S_{21} between the data and yield terminals of the exchanged circuit, under the no-transmission state or when the switch is in the off condition. A vast worth (in decibels) shows little coupling in the middle of data and yield terminals. Therefore the outline objective is to boost the isolation. In RF MEMS switches isolation may debase as a consequence of closeness coupling between the moving part and the stationary transmission line as an aftereffect of spillage currents.

(ix) Series resistance

In many instances, the switch is connected in series with the transmission path. Any resistance offered by the switch during signal transmission (on state) would result in loss of signal level. One way of representing this, especially at lower frequencies, is to use the series resistance of the switch while it is conducting. At higher frequencies, this is often represented by the insertion loss.

(x) Actuation voltage

All automated systems require a control signal for actuation. Depending on the scheme and its efficiency, these voltages vary significantly. Although this is not a big problem with semiconductor based switching systems, one of the design objectives of state-of-the-art electromechanical switching systems is to bring down these voltages to levels compatible with the rest of the circuit.

(xi) Life-cycle

This is also not a significant issue with semiconductor-based switches, but in all schemes that involve moving parts, the lifetime may have to be considered. The breakdown of such moving components because of fatigue and environmental effects limits the lifespan of these systems as concluded by Li (2003).

(xii) Resonant frequency

The moving parts in mechanical switches have resonant frequencies that can be modeled in terms of their effective spring constants and resonating mass as described by Saha (2009). At this frequency, the potential energy and the kinetic energy tend to resonate. This frequency limits the maximum rate at which the switch can be toggled, but this virtually has no bearing on the frequency of the actual RF signals the switch carries. In electrical circuits, resonance occurs when the reactance of an inductor balances with the reactance of the capacitance for a given frequency. In a resonant circuit, when it is in series resonance, the current will be at a maximum, offering minimum impedance and vice versa in parallel resonance.

(xii) Intercept points

The intercept point is the extrapolation of the distortion power to the power level of the drive signals, assuming the switch has no compression of the signals. It is usually assumed that the intercept points are related to the frequency of the minority carrier's lifetime in PIN diodes. The ratio of the stored charge to diode series resistance is the common driving factor in PIN diode distortion.

(xiii) Phase and amplitude tracking and matching

Phase and amplitude matching specifications are important in multi-throw switches since, depending upon the design of the devices. The individual throws can have different electrical lengths and losses. This will result in different phase and amplitude characteristics for each throw.

1.6 SWITCHES FOR RF AND MICROWAVE APPLICATIONS

The main uses of RF switches in the telecommunication industry are for signal routing, in impedance matching networks and for changing the gain of amplifiers. Telecommunication covers a broad range of frequencies, from below HF through VHF. Several new applications at frequencies in the microwave and millimeter wavebands are also well established. These include AM band (at the low end of MHz), commercial FM band (88–108MHz), military handheld radio transceivers and cellular radios (900MHz and 2.4GHz) and Bluetooth (2.45GHz). In addition to these, there are also other applications at frequencies ranging from Ku-band (12.4–18GHz) to the upper side of W band (75–110GHz), which require the use of high-quality RF switches. Yao, 2000 discussed that the wide frequency spectrum used for telecommunications demands different switch technologies for various frequency bands of application. Furthermore, increased use of personalized communication terminals requires downsizing of mobile systems and their accessories. Along with varying frequency requirements, the power handling capability of the device may also differ for various applications. In the case of silicon FETs, for example, it can handle high power at low frequency, but the performance drops off dramatically as frequency increases. In the case of GaAs metal–semiconductor field effect transistors and PIN diodes the high-frequency operation is fairly well with small signal amplitudes. In short, when the signal frequency is greater than a few Gigahertz these solid state switches have large insertion loss (typically1–2dB) and poor isolation (~−20to −25dB). The need for an alternative switch is inevitable and MEMS exhibits promising characteristics as the new technology for integrated switching devices. The selection of a switch largely depends on the signal level and speed of operation that the application demands. Both mechanical and solid-state switches have their own

advantages and disadvantages. Owing to the integration compatibility and low manufacturing cost, most present switching techniques for RF and microwave applications are met by the solid-state semiconductor devices. This section is therefore intended to present different RF switching systems in perspective, before discussing the RF MEMS switches themselves.

1.7 MECHANICAL RF SWITCHES

Electromechanical switches have been widely used for high-power applications in TV, AM, FM, HF and other broadcast systems. Owing to the high power, these devices are made available with either waveguide or coaxial connector ports. Electromechanical RF and microwave switches with various specifications and frequency bands are available from several commercial vendors, 2 for power levels ranging from kilowatts to megawatts. The low-frequency coaxial switch from Micro Communications (Manchester, NH) can handle 1500kW peak power from dc to 800MHz. The space programs Pathfinder, Geosat, Immersat III and Intelsat are a few examples of where Dow-Key (www.dowkey.com/products/) microwave switches are used. An extensive list of manufactures offering high-frequency switches is provided in the microwave and RF product data directory (www.mwrf.com/products/). The selection of the RF switch for a circuit depends mainly on the type of platforms and applications. Mechanical switching is done through a make or break in the transmission line or electrical path by a control signal activating an electromagnetic relay. These mechanical switches can be designed to turn on and off in different ways. For example, in a latching design the switch remains in a preselected position when the actuating voltage is removed, holding the switch in that position until the next actuating voltage is applied. Accordingly, some switches are built normally open with all output ports disconnected from the input until the actuating voltage is applied. In other designs, the switch port opens with the actuation voltage and returns to the predetermined closed position upon the removal of the voltage. A typical fail-safe electromechanical switch uses an electromagnet for actuation to move an arm, and a spring to pull it back to the initial position. Such a switch is always in the normal position until the application of current to the coil actuating it. The switch returns to the normal position as the power is removed from the coil. Loh (2011) developed an identical device and this device finds several applications where the switch should be in the normal position in the event of a power failure. In many switching configurations, when the switch is off (or the electrical path open), there is no alternative path for the RF power to propagate. To prevent high RF power from reflecting back to the source in such instances, circulators or coupling devices must be incorporated in the design to direct the

RF energy to a dummy load. Internal terminations, generally 50Ω resistors, are added to the switch ports to absorb the RF power while the electrical path is interrupted. Even though many of these electromechanical switches exhibit excellent RF characteristics such as low insertion losses and high isolation, typically up to several hundreds of megahertz, they have a very slow switching speed. In general, these switches are operating at a speed of 2 to 50ms and are rated for several million switching operations. This is because the switching is performed by physically blocking or opening the transmission path in a device. The mechanical resonant frequency of these moving parts determines the maximum frequency of operation (switching speed) of these devices. For higher-speed operation semiconductor-based switching devices, discussed next, are preferred.

1.8 ACTUATION MECHANISMS FOR MEMS DEVICES

Advances in micro and nano fabrication techniques influencing the outlook of MEMS. Recently, a microelectromechanical system has been defined as a miniature device or an array of combined electrical and mechanical components fabricated with IC batch- processing techniques as per techniques used by Yang (2010). The key advantage of the MEMS device is its ability for bulk reproduction and batch fabrication. Most mature fabrication technologies such as bulk micromachining and most recent techniques such as LIGA have their own merits and demerits while adapting for MEMS fabrication. It is still early for a time-tested categorization of RF MEMS devices because the development of MEMS devices for RF applications is yet to mature. For the RF design engineer, even though the MEMS devices are mechanically actuating with prescribed electric fields, it gives clear demarcation in the functionality inside the RF circuit. In an RF circuit, switching devices such as bipolar junction transistors (BJTs) or FETs can be replaced with MEMS switches or it is possible to use the MEMS device to re-route the RF signal between different transmission paths. However, in many RF circuits, the most important consideration should be its reactive elements and the induced inductive or capacitive elements because each has their own clear operational functions in an RF circuit. The actuating and control circuits should not load the circuit, and the dc voltage has to be isolated from the RF path. The actuation of the switch can be electrostatic, magnetic or electromagnetic: each has its pros and cons. The advantage of electrostatic actuation is that there is no current consumption; its drawback is that it requires a higher actuation voltage, typically 5–100V. The advantage of electromagnetic actuation is the lower voltage, but, with significantly higher current consumption. Electrostatic switches offer the most promise as configuration switches, where low power consumption is the key factor.

CHAPTER 2: LITERATURE REVIEW

2.1 INTRODUCTION TO RESEARCH MODEL

In this research, model is being newly invented and there is a vast area for new inventions and optimizations, so far there have been numerous researches and evaluations of the same and by employing the survey of various research papers, it has been found out that variations in design, geometry, switching speeds, air damping and axial forces have a great impact on various properties of the MEMS switches and the base, Tripp (2006). Such variations are to be explored more and more as there are an infinite number of ways to employ Finite Element methods for this topic to reduce the stress gradient or better reliability.

2.2 LITERATURE REVIEW

Holemberg et al. (1998) presented the fast development of a large variety of different advanced surface modification and coating deposition techniques during the last few decades offers remarkable possibilities to improve the tribological properties of surfaces and thus improve the functional reliability and lifetime of tools, components and other surfaces in sliding contact. Full advantage of these developments can only be achieved when appropriate methods for surface design and optimization are available. To support this, a systematic approach to the analysis of tribological coated surfaces has been outlined. It is based on a classification of the tribological contact process into macro-, micro- and nanomechanical and tribochemical contact mechanisms and material transfer. The use of thin multilayers offers an excellent possibility for surface design to achieve the required proper- ties at the surface. Increased coating/substrate adhesion, improved load support, surface stress reduction and improved crack propagation resistance can be achieved by different concepts of multilayer surface design. From a tribological point of view, the diamond and diamond-like hard carbon coatings represent the most dramatic new coating concept introduced during the last few decades. In dry sliding the friction can be extremely low with a coefficient of friction of less than 0·01 and a wear resistance more than one order of magnitude better than for any other hard coating. The diamond-like coatings can also be used with good tribological performance in oil- or water-lubricated conditions with some care. For example, hydrogenated diamond-like coatings may show catastrophic failure when sliding in water environment while hydrogen- free DLC coatings perform well.

Tanner (2000) inspected the real victories in diverse MEMS gadgets from an unwavering quality perspective. The dependability issues of a mixed bag of MEMS gadgets, (for example, weight

sensors, ink-plane print head, micro-mirror clusters, and RF switches and resonators) were talked about. It was presumed that the MEMS items are satisfying desires as far as execution, expense, and dependability. Some of the major MEMS concerns have been addressed in this review. The major concern for these small devices is stiction, which affects yield and reliability. Wear and the resulting adhesion that causes failure has been shown to be a dominant reliability issue. Fracture has not been observed much, but the work to characterize materials properties is essential to provide values for design calculations. Fatigue is not an issue as of yet for polysilicon, but it may be a concern for other materials. MEMS devices have demonstrated robustness to shock and vibration, although combinations of effects (e. g. out-of-plane shock which causes stiction) may indeed be a concern.

Li and Bhushan (2002) developed a technique to perform bending and fatigue tests of nanometer scale fixed beam specimens made of single- crystal silicon using a depth-sensing Nano indenter with a harmonic force has been described. The Nano scale beams exhibited higher bending strength than the larger scale specimens. Load cycles used in the CSM were used to study the fatigue properties of Nano scale Si beams. Fatigue behavior of the beams was monitored by a change in the contact stiffness. Cleavage steps were found on the fatigue fracture surface. The nano indentation bending and fatigue tests used in this study can be satisfactorily used to evaluate the bending strength and fatigue properties of Nano scale structures for use in MEMS.

Bhushan (2003) presented a very important review regarding causes of stiction and adhesion, along with methods to reduce the stiction and different measurement techniques in commercial ME Sand magnetic storage devices. Several techniques for adhesion measurement, i.e., surface force apparatus, atomic force microscopy (AFM), micro-triboapparatus, and cantilever beam array, were addressed. Adhesion between solids arises from the interatomic forces exerted across the interface. These forces may be strictly surface forces in the sense that they derive from the surface atoms themselves. Valence bonds provide surface forces. Surface charges also provide surface forces; these occur when ionic surfaces are in contact with other ionic solids. They will also occur if an electrically charged layer is formed at the interface, e.g., during sliding ~the triboelectric effect! Metallic bonds can form primarily in metal–metal pairs. All solids will, in addition, experience adhesion due to van der Waals interactions between atoms below the surface layers. Hydrogen bonds can occur in polymers. Adhesion interactions may often be calculated in terms of free surface energies. The energy required to create new surface, ex- pressed over an area consisting of many atoms in the surface lattice, is referred to as the free surface energy. The higher

the surface energy of a solid surface, the stronger the bonds it will form with a mating material. One obvious suggestion is to select materials that have a low surface energy. The use of lubricants at the interface reduces the surface energy. Ma- terials with low work of adhesion result in low adhesion, where work of adhesion represents the energy that must be applied to separate a unit area of the interface or to create new surfaces.

Yapu (2003) presented a survey on stiction and hostile to stiction research for MEMS gadgets. A few test perceptions of stiction in micro-machined accelerometers and RFMEMS switches were exhibited, and some criteria for stiction of micro- and Nano-structures in MEMS and coming about because of surface powers were examined. The effects of surface harshness and natural conditions on stiction wonder and strategies to diminish stiction in MEMS and were inspected also. The extremely high surface-to-volume ratio of MEMS makes interface stiction, friction and wear significant factors in determining device reliability. These important problems must be solved in a near future for production of reliable and long lasting MEMS. Some criteria for stiction of microstructures with substrate have been reviewed in this paper. Though some physical models have been established, great efforts including experiments, molecular dynamics (MD) simulation and theoretical analysis are still needed to better understand the mechanisms of stiction, jump-in-contact (JC) and jump-out- of-contact, and adhesion hysteresis.

Srikar et al. (2003) suggested that microsystems (MEMS) technologies are evolving at a rapid rate, with increasing activity in the design, fabrication, and commercialization of a variety of different micro scale devices and systems. The successful fabrication and reliable operation of structures with feature sizes in the range 1 (μm to 1 mm requires accurate mechanical property measurement at these length scales. In this paper, we have reviewed micro scale mechanical testing from the point of view of the engineer engaged in MEMS design. In particular, he have (i) identified the mechanical properties of interest for the de- sign of microsystems, (ii) cataloged and critically compared the various test techniques, and (iii) suggested a rational approach for the selection of test methods for microsystems de- sign. The details of specimen preparation, experimentation, and data analyses are contained in the cited literature.

Zhu (2004) proposed a study that because of some application prerequisites and the gadget bundling, there is a critical requirement for comprehension the effect of RF MEMS switch outline on its execution as a capacity of temperature. High temperatures may cause clasping of the switch structure, which would prompt gadget disappointment. By difference, low temperatures may bring about an undesirably high draw in voltage that can trade off the gadget life by charge assemble up

or lead to other disappointment modes. This article tends to this issue by examining demonstrating and experimentation approaches and, specifically, by breaking down a promising anxiety unwinding structure in light of film folding. Due to some application requirements and the device packaging, there is an important need for understanding the impact of RF MEMS switch design on its performance as a function of temperature. High temperatures may cause buckling of the switch structure, which would lead to device failure. By contrast, low temperatures may result in an undesirably high pull-in voltage that can compromise the device life by charge build-up or lead to other failure modes.

Bhushan et al. (2006) presented a comparative study for the Nano scale friction and adhesive properties of various SAMs with different hydrocarbon backbone chains (DP, ODP) and fluorocarbon backbone chains (PFDP) deposited via chemisorption onto an Al substrate. The influence of environment (RH and temperature), sliding velocity, and wear was studied, and the corresponding friction mechanisms were discussed. Both fluorocarbon and hydrocarbon SAMs showed a reduction in adhesive force, friction force, and coefficient of friction as compared to bare Al. PFDP, which has the lowest surface energy, also exhibited a lower adhesive force than either of the hydrocarbon SAMs. At small normal loads, the friction force for fluorocarbon was lower than for hydrocarbon SAMs. However, for high loads, the friction force was higher for fluorocarbon compared to hydrocarbon SAMs. The SAMs deposited on the Al substrate showed a negligible dependence of adhesive force on the RH. However, there was some decrease in coefficient of friction. This effect could be attributed to lubrication by the adsorbed water layer. The adhesive force for SAMs with a hydrocarbon backbone chain shown temperature dependence. The adhesive force for SAMs with a fluorocarbon backbone chain, on the other hand, was temperature independent over the temperature range studied. The friction force for the SAMs on Al also showed little dependence on the sliding velocity. The SAMs with a fluorocarbon backbone chain showed much larger friction force, as well as, a larger sliding velocity dependence. Wear behavior of the SAMs is mostly determined by the molecule–substrate bond strengths. The long hydrocarbon chain molecules of ODP and the fluorocarbon backbone chains of PFDP showed higher critical loads than DP with its short hydrocarbon chain molecules and bare Al. From a tribological point of view, it is found that SAMs with compliant and long hydrocarbon backbone chains and those with fluorocarbon backbone chains show a highly desirable behavior. This study is expected to aid in the design and selection of appropriate lubricants for MOEMS/NOEMS on aluminum substrates.

Changhong (2006) described the functioning of a two-terminal nanotube based nanodevice with a closed-loop feedback control mechanism was experimentally demonstrated by in situ SEM testing. An electromechanical analysis was employed to interpret the experimental current–voltage measurements. Both experimental and theoretical modeling demonstrated the bistability of the device, which can be employed advantageously in applications such as memory elements, NEMS switches, and logic devices. Shortening of the nanotube cantilever was observed in the experiments during the pull-in process. Stress-wave-induced CNT fracture as a result of mechanical impact during the pull-in event was proposed to account for such device failure, which was sup- ported by a separate in situ SEM experiment. The failure mechanism shows that in order to design reliable NEMS de- vices, it is imperative to gain a fundamental understanding of failure modes as a function of configuration parameters. Ultimately, maps defining regions of robust device opera- tion need to be developed. Various failure mode and mechanism analysis, manufacturing Reliability, aging and degradation models, failure and lifetime models, Reliability testing, evaluation and measurement techniques, as well as structure and parameter design techniques for Reliability of Nano-devices were reviewed. The behavior of nano-scaled products is much more sensitive to changes in material compositions, manufacturing control- lable variables, and noise parameters.

Grothi et al. (2006) proposed that cantilever beam electrostatic actuators with an intermediate dielectric layer have been analyzed in detail over the entire operational range using a beam model. The results are validated with the 3D simulation results from CoventorWareTM. Three qualitatively different configurations, here called floating, pinned and flat, have been identified and studied. A scaling law is found for the flat configuration. Transitions from and to the floating configuration (pull-in and pull-out)and transitions from pinned to flat (pull-down) and flat to pinned (pull-up) have been studied as well. Bi-stable and tri-stable states have been found. A classification of all possible types of transitions is made based on the dielectric layer parameters. Dynamic stability analyses have complemented the study of these configurations and transitions. Higher dielectric thickness gives more regular and predictable behavior at the cost of lower overall tenability in device characteristics.

Wei et al. (2006) presented finite element formulation which accounts for surface elasticity has been derived from the potential energy functional to describe the size dependence of the mechanical properties in Nano systems. Its validity has been verified from the stress concentration at a Nano void. The newly developed surface element has then been applied to the investigation of

surface effects in the interaction between Nano voids and the effective moduli in nonporous materials. Some valuable mechanical and physical behaviors of Nano systems different from the classical elasticity are studied in detail. Numerical results for the interaction between two Nano voids show that the interaction intensity is enhanced or weakened with decreasing void radius for a given ratio of D/R; the surface effect also has a significant influence on the effective properties of Nano porous materials. It should be noted that the surface element developed in this paper is reliable and can conveniently facilitate the study of surface elastic effects in many other Nano sized problems, for instance the mechanical response of some nonstructural elements such as Nano beams, Nano bars, nameplates etc. Meanwhile, the idea of our derived surface element can be generalized to study the effects of the interface by developing a kind of interface element, if the interface elastic constants are known. Finally, as mentioned above for some problems the large absolute value of negative surface modulus brings about an ill conditioned total stiffness matrix, therefore effective numerical methods to deal with the ill defined problem and improve the precision of solutions are worthwhile to include in future work..

Saha et al. (2007) adopted a study of comprehensive analytical model for non-uniform cantilever. The model matches quite closely with the Coventor-Ware simulation result. The ratio between the model and Coventor-Ware result is almost constant for different electrode widths. When the cantilever is longer (200 Pm) the spring constant is very low and the electrode width has very low effect on spring constant. This will reduce the pull down voltage as the actuation force is higher. This model will be very useful for predicting pull down voltage of non-uniform cantilever. This model can be implemented by any simple mathematical tools and calculation can be done within very short time. We have made a comprehensive analytical model for non-uniform cantilever. The model matches quite closely with the CoventorWare simulation result. The ratio between the model and CoventorWare result is almost constant for different electrode widths. When the cantilever is longer (200 ptm) the spring constant is very low and the electrode width has very low effect on spring constant. This will reduce the pull down voltage as the actuation force is higher. This model will be very useful for predicting pull down voltage ofnon uniform cantilever. This model can be implemented by any simple mathematical tools and calculation can be done within very short time.

Bhushan (2007) presented an analytical review on Nano tribology and Nano-mechanics of MEMS and Bio MEMS/Bio materials and devices. Micro/Nano scale adhesion, friction, and wear studies of materials, lubrication studies, and component-level stiction phenomena for aforementioned

devices were reviewed. It was concluded that adhesion, stiction/friction, and wear reduce the lifetimes and thus the Reliability of MEMS/ and Bio MEMS/ Bio devices. The tribological needs of these devices were addressed as well.

Jeong et al. (2009) framed a 3-T NEM switching device 700 nm in length with a 40 nm air gap was developed using a CMOS compatible process and was tested in transformer oil. By utilizing a liquid medium, the operation voltage could be reduced and the reliability was improved dramatically owing to a reduction of surface adhesion force, suppression of arcing, and prevention of exposure to moisture/oxygen. The device shows improved number of reliable switching and a reduction in operation voltage (40%) with liquid medium packaging.

Mustafa et al. (2009) made conclusions taking into account investigation of the vibration modes and the first mode is the best for building up a capacitance-based MEMS current sensor. The estimation of the recurrence of the first mode decided from recreations compared well with the worth figured from the model, and the minor distinction could be credited to the distinctive systems utilized as a part of the product rather than the systematic model. The regular recurrence of the small scale cantilever was high contrasted with the recurrence of the signal current at just 50 Hz. In this way the impact of the regular recurrence on the amplitude of the movement is little. A direct relationship between the proportion of capacitance change and the amplitude of the movement (because of a connected magnetic field) was indicated. A higher affectability can be acquired by planning ideal beam measurements and this was recreated with predictable results.

Groot et al. (2009) presented a review on failure mechanisms (such as leakage and different types of stiction) due to use of dielectrics in electrostatically driven MEMS devices. Moreover, methods and techniques to characterize the material properties and effects on Reliability of these devices were reviewed. Dielectrics play a versatile and often crucial role in MEMS devices. Both conventional SiO2 and SiN and higher k materi- als are under exploration in experimental MEMS varactors and RF switches. The advantages of the large-capacitance tuning range made possible with high-k dielectric MIM devices and the reduction in parasitic capacitance due to thicker dielectrics are making high-k dielectric materials attractive for a range of MEMS applications. Improvements in process technology will advance throughput of deposition processes and dielectric quality for these dielectrics and facilitate implementation and commercialization. Extensive reliability testing is still needed to evaluate standard reliability issues such as tunneling, charge trapping, and breakdown strength, as well as properties such as surface energy, hardness, permittivity, and refractive index.

Jau (2009) measured and analyzed the RF performance and hot-switching Reliability of an RF MEMS switch mounted on a PCB. He added an external circuit to improve the hot-switching Reliability of the MEMS switch. However, there were trade-offs for the addition of the external circuit in terms of insertion loss and return loss. One can use the information in this paper to determine the suitability of RF MEMS switches in our application from the perspectives of high-frequency performance, as well as hot-switching life cycles under different signal conditions

Yang et al (2011) revealed the importance of employing non-roughening for reliable hermetical capsulation of MEMS manufacture. The surface roughening is realized via a no uniform etch characteristic of PR which is etched then utilized as an etching mask for the following silicon etching process. The roughening can not only enhance adhesive bonding strength and hermetic encapsulation yield for N/MEMS manufacture, but also provide better sticky characteristic possible for Nano imprinting applications.

Fonseca et al. (2011) discussed and reviewed the Reliability issues in the context of MEMS functionality. They also briefly reviewed the failure mechanisms for MEMS devices. Dielectrics also play a crucial role in performance and Reliability of MEMS/ devices.

Zaghloul et al. (2011) explored and investigated the examination work completed in basic disappointment instruments of electrostatic MEMS and, i.e., the dielectric charging and stiction phenomena. The paper talked about late Nano-scale portrayal strategies and the effects of relative stickiness and dielectric testimony conditions on the charging and releasing methods, Zhao (2003). The Nano-scale portrayal results exhibited a significant relationship with the gadget level estimations. Albeit each of the past papers evaluated alternate points of view of MEMS/ dependability, none of them coordinates different unwavering quality issues for MEMS/ gadgets. This paper means to fill the hole by auditing late papers on MEMS/ unwavering quality and examining them in three classifications: disappointment modes and systems, dependability issues in outline and assembling, and unwavering quality assessment and testing.

Basu et al. (2012) described about MEMS cantilever beam altered toward one side being used for acknowledging recurrence doublet. The microstructures have been composed and created utilizing a surface micromachining process, and have likewise been limited component recreated for their mechanical reaction. Hypothesis and reenactment have been found to match well. Further, the usefulness of the recurrence multiplying gadget has been tentatively exhibited utilizing LDV strategy for two created cantilever beams. The testing has been rehashed on gadgets on different passes on. The test outcomes have been discovered to be in sensible consistence with the evaluated

results. The work reported there can be further proceeded with different prospects, including the quick execution examination of MEMS recurrence doublet with tantamount semiconductor variants, and the use of high-recurrence mass mode resonator geometries for recurrence multiplying applications.

Fior et al. (2012) suggested that the aim of research was the realization of transparent and versatile bio-MEMS for the evaluation of the mechanical properties of single living and adherent cells. The first step was the design of structures, validated and integrated through finite element modeling. The choice of materials played a fundamental role, in particular because high transparency was a strict requirement for this MEMS. The production technique was devised using clean room facilities for thin film processing. Good structural results have been achieved. Structures have been characterized and a high transmittance and optimal refractive index are shown. The final result is bio-MEMS which can be used in a liquid environment for testing single living cells in adhesion.

Huang et al. (2012) carried out work stated the reevaluated work of van Spengen's review by revising the failure mechanisms in MEMS, such as fatigue, fracture, wear, creep, stiction, electrical failures, and contamination was proposed. Further, analysis of the effects of failure subjects on performance of devices, and the steps to be taken in order to reduce the failure rates were devised. The fast development of a large variety of different advanced surface modification and coating deposition techniques during the last few decades offers remark- able possibilities to improve the tribological properties of surfaces and thus improve the functional reliability and lifetime of tools, components and other surfaces in sliding contact. Full advantage of these developments can only be achieved when appropriate methods for surface design and optimization are available. To support this, a systematic approach to the analysis of tribological coated surfaces has been outlined. It is based on a classification of the tribological contact process into macro-, micro- and Nano mechanical and tribochemical contact mechanisms and material transfer.

Passi et al. (2012) proposed a new process for fabricating Si NWs and ribbons under large strain has been developed and applied to 50- and 500-nm- wide specimens with lengths varying of 2.5, 5, and 10 μm, and series of nanoscale tensile tests were performed on monocrystalline Si NWs and nanoribbons to evaluate the statis- tics of fracture. The increase of the fracture strain for decreasing specimen volume is observed, indicating the reduction of defect density in the volume of silicon. The probability of survival versus deformation has been calculated, showing that 100% of samples fail at $\varepsilon>5\%$ and 70% of samples resist $\varepsilon<3\%$. A two-parameter Weibull distribution was performed which characterized the strain distribution for the nanoribbons and nanowires. The main

advantages of the aforementioned method are as follows: 1) high throughput; 2) reproducible large strains > 3% are attained for the narrowest nanowires; and 3) electrical characterization of the devices can be easily integrated with the method to determine piezoresistance effect in Si NWs at high strain values.

CHAPTER 3: METHODOLOGY

3.1 PROBLEM FORMULATION

This chapter is describing the process of design and modelling of RF MEMS switch. The procedure for the framing of design feasibility and modeling through software is developed as well as shows the mathematical relations on MEMS cantilever shunt switch. After literature reviews, the following problems are to be formulated:-

- Adhesion problem which is generally occurring during the cantilever switching operation.
- Due to very minute size, the load is much more at the edges of switch.
- The material intra reactions are occurring because of the heat produced during switching operation.
- The regular switching operation causing the fatigue to generate at the sharp edges and ultimately causing the failure of the beam.
- Since very reactive materials are used for the dielectric and the substrate applications, the switch is likely to get corroded by the external attacking agents of nature.

3.2 RESEARCH GAPS

The following are the various unidentified parameters detected from the various researches:

(i) The most of designs of contacting strip has never been modified for a feasible functionality in varied designs of the MEMS switches mechanisms such that the switch has a longer life and better reliability.

(ii) Most of the previously designed switch exhibits large areas of stress concentrations which have never been modified for reduction of stress gradients such that there could be more actuations cycles than the primitive switches.

(iii) Thermally stable MEMS devices have never been used with heat dissipating elements to reduce the thermal instability.

(iv) Transmission line has never been used as for a switching mechanism.

(v) Being the very common problem of the adhesion and stiction has never been coped with employment of a point contact surface to reduce the contact area in such a way that the material loss is much lower.

3.3 OBJECTIVES

The following are the objectives identified from the various research gaps obtained from the research papers:

(i) To propose and design a rigid cantilever beam with heat dissipating properties for shielding the switch.

(ii) To design a low stress concentration switching mechanism with a hybrid combinations of crab leg and serpentine flexures.

(iii) To reduce the contact area by using point contact surfaces for the contact strip by employment of small conical contact points.

(iv) To obtain working RF MEMS switch with novel design having increased reliability and reduced stress concentration is obtained.

Design, Modelling and analysis are done using computer aided software support by COMSOL, ANSYS-HFSS and AUTOCAD, PRO-E or CATIA.

3.4 MECHANICAL SWITCHES

The examples of mechanical switches are toggle switches, push-button switches, relays, etc. In relays, the electromagnetic force arising from the flow of current through a coil causes a metallic contact physically to open or close.

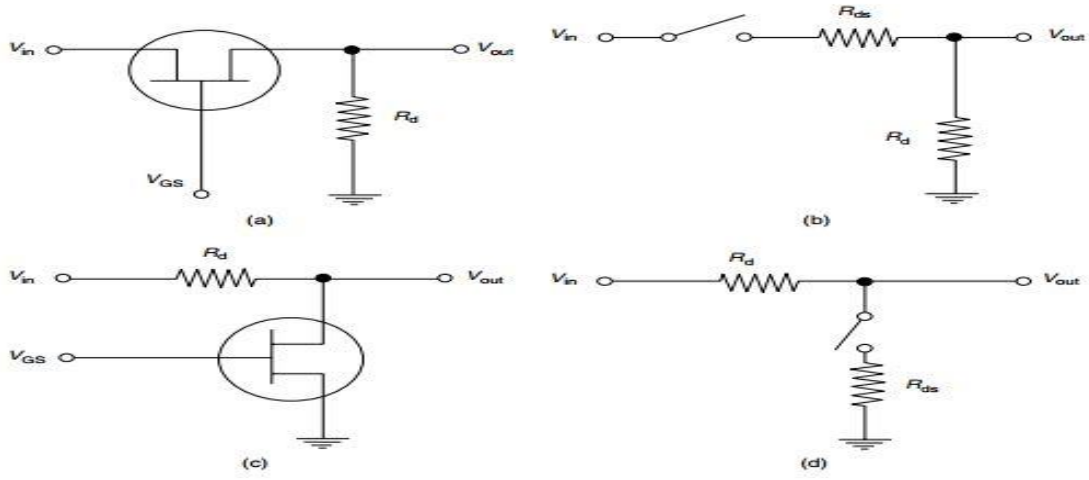

Figure 3.1: Typical Configuration of FET (Field Effect Transistor) Switching Circuits (Vardhan, 2003)

(a) Series Switch; (b) Series Switch Equivalent Circuit; (c) Shunt Switch; (d) Shunt Switch Equivalent Circuit

[Note: V_{GS}, gate voltage; V_{in} and V_{out}, input and output voltage, respectively; R_d, R_{ds}, bias resistance of the circuit and the drain-source resistance of the FET, respectively]

The most widely used switching elements are armatures and are available in various forms for a wide variety of specifications. Because of the physical movement of the contact points, the relays suffer from low lifetime, Fonseca (2011) studied degradation of electrical contacts and mechanical wear out. All these cause a very high rate of failure in operation.

3.5 DYNAMICS OF THE SWITCH OPERATION

The cantilever consists of a thin strip of metal and dielectric that is fixed at one end and suspended over a free space. If the thin metal and the dielectric is fixed at both ends and suspended in middle, the structure is a bridge. In a diaphragm, the thin membrane of metal and dielectric is fixed around its periphery and suspended at the middle. In all these configurations, the structures are suspended over a bottom metal electrode so that a capacitor is formed. When the bias voltage is applied between contacts, charge distributes in such a way that an electrostatic force occurs between them, independent of the voltage polarity. This force pulls the top electrode towards the bottom one creating an opposing tensile force as the structure is bent. When the applied force reaches a certain threshold value, the tensile force no longer balances the electrostatic force and the cantilever abruptly falls to the bottom contact. Figure 3.2 presents a schematic diagram of the capacitive bridge RF MEMS switch modeled as a fixed-fixed beam identically used by Zhu (2004). This model gives an approximate solution for the nonlinear differential equation, which is difficult to solve in general.

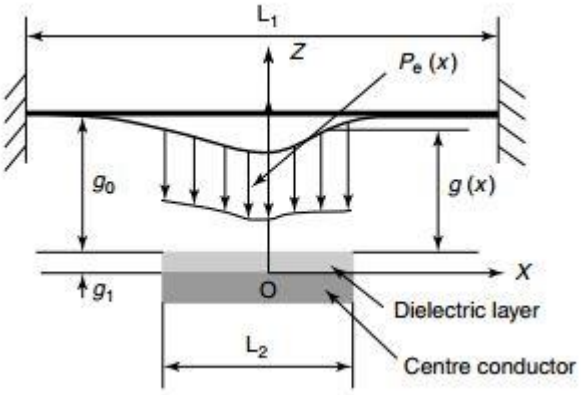

Figure 3.2: RF MEMS Capacitive Switch Structure Modeled as a Fixed-Fixed Beam (Reibiz (2003)

[Note: L_1, L_2, g_0, g_1 and g_x are as defined here; $p_e(x)$ is the equivalent load on the cantilevers a result of the applied electric field]

3.6 EXPERIMENTAL MEMS MODELING, SWITCH DESIGNING AND EVALUATION

One of the significant challenges limiting design and commercialization of RF MEMS products is RF systems developers' own computer-aided design (CAD) tools. The challenge is to bring the integrated designs together with numerous analog and mixed signal microelectronics blocks and MEMS components on a single chip or assembled in an integrated package as depicted by Liu (2012). Silicon micro machined structures, despite using IC processing techniques, are no less complex than structures like bridges. Success in fabricating and utilizing them is tremendously complicated by their small size and impossibility of using many traditional mechanical diagnostic methods. Although the recent system-on-chip (SoC) methodologies have triggered efforts in top-to-bottom integration, MEMS design is a different discipline that traditionally has required tedious manual design techniques and in-depth understanding of the fabrication procedures. The lack of common platforms for sharing the design information increases the likelihood of serious design flaws and adds additional iterations. For example, the automatic transferring of the information derived from the 3D field solvers on MEMS structures should be compatible with state-of-art IC design tools. MEMSCAP's MEMS Component library available for the popular Agilent Technologies Advanced Design System (ADS) design platform is an effort towards the realization of this challenge. These libraries provide different views such as functional views with S-parameters, electronic views with Spice model, implemented on various CAD platforms enabling the design on functional RF MEMS components. Saha (2007) showed that he designs of these components are achieved using full-wave electromagnetic simulation based on the finite element method (FEM). The FEM analysis allows modeling of the complete structure, including the different layers and properties of the material with a parameterized description of the components. Attempts have been made to develop fully integrated FEM-based packages to model the behavior and fabrication process dependency of MEMS devices, which has to consider the physics of the components and geometry effects due to etching, along with material dependence. Mechanical design plays a crucial role in the electronic integration of MEMS devices. The mechanical design could influence the device as well as system performance, although the design techniques may vary based on specific MEMS applications. Li (2014) designed one of the conventional MEMS design starts with either a two-dimensional (2D) layout and later adds the parts based on the fabrication process to generate the 3D model, or a 3D model can be directly created using a 3D design tool, which should be compatible with the fabrication process. The Coventor's Designer software used by Li (2014), meshed solid models for physical analysis can automatically be

created from the 2D layout. Later FEM analysis can be used to mechanical optimization of the design. The analysis can be done using Analyzer. Figure 3.3 highlights the effect of the impact of physical distortion on the performance of a MEMS device. The distortion, which is shown by the shading difference, is caused by the residual stress. The impact of distortion on the RF performance will vary based on the application. However according to Li (2014), it is important to consider when designing the switch. Coventor's design methodology provides the ability to analyze distorted and undistorted devices. The software also provides the ability to use a structured custom design approach, starting with the system level of MEMS devices to evaluate their behavior and to converge to the optimized design. The interaction of these MEMS devices with the surrounding electronic circuitry is also important and the software provides the ability to analyze the environmental effects, signal conditioning and packaging. This evaluation will help to refine the MEMS design as well as the design of the control circuitry in the subsystem.

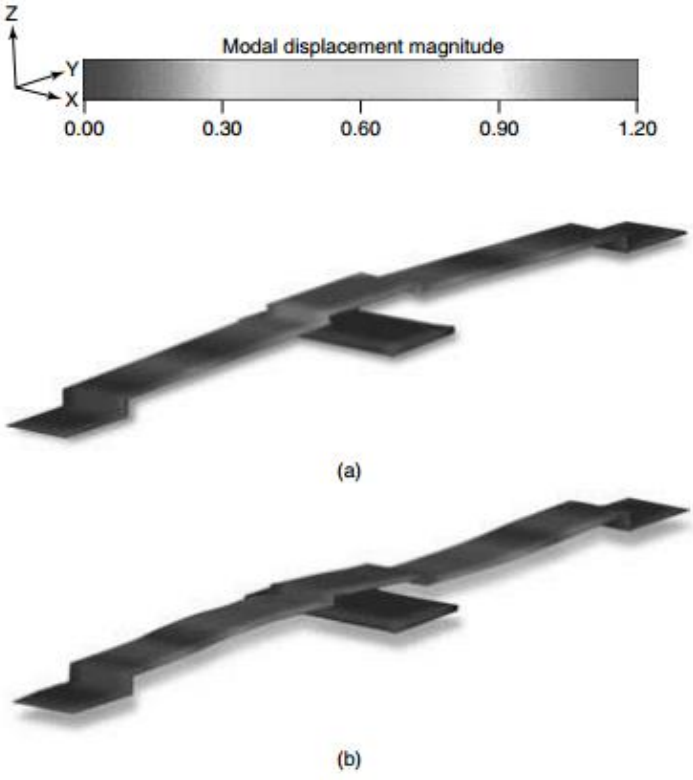

Figure 3.3: Model of (a) Undistorted and (b) Distorted Switch (Vardhan, 2003)

3.6.1 Electromechanical Finite Element Analysis

In-depth finite element analysis of the design of a cantilever switches were performed using Ansys with the geometry and element mesh shown in Figure 3.4 (a). The gold layer is 1.0 μm thick and is suspended below and overlapped by silicon nitride layers 0.8μm thick. The magnitude of the pressure applied is related to the applied voltage, which increases as the electrode deflects

downwards. The anchor point of the armature is fixed in space with no translation or rotation. Figures 3.4 (b) and 3.4 (c) show the fully fixed conditions for these nodes.

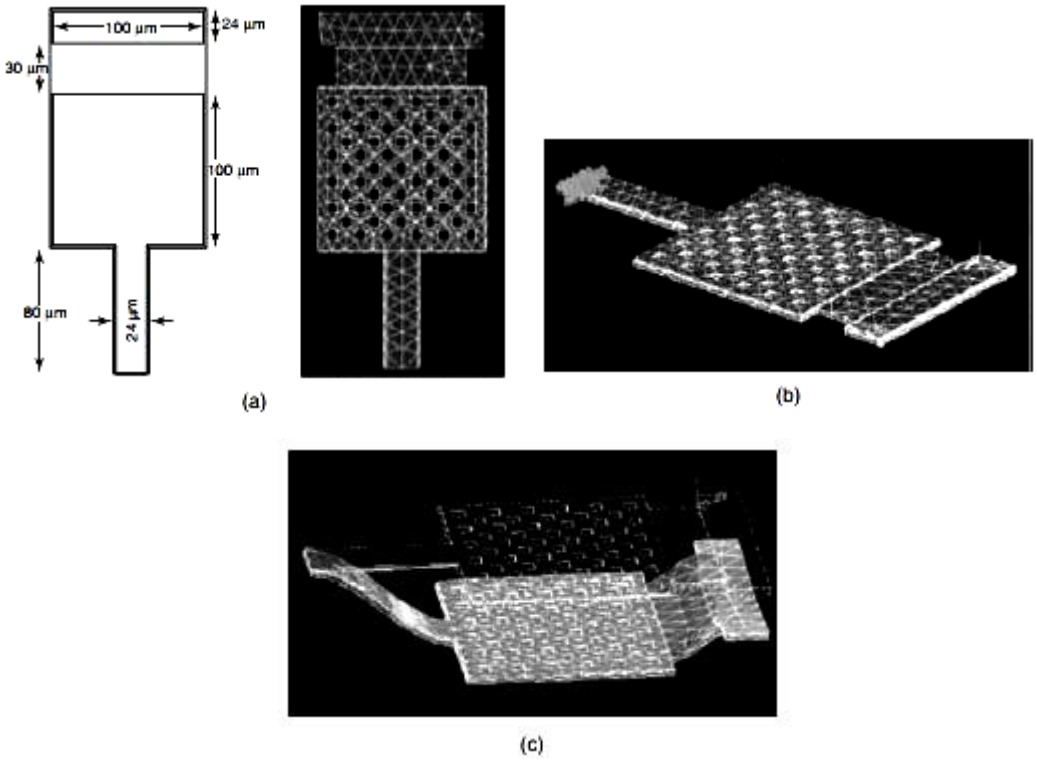

Figure 3.4: (a) Geometry, Dimension and Meshing of Finite Element Method (FEM) of MEMS Switch (Reibiz, 2003) The Gold Layer is 1µm Thick and The Silicon Nitride Layer is 1µm Thick. (b) Isometric View of the Fem Mesh of the MEMS Switch Showing the Application of Electrostatic Pressure over Area of Bias Electrode. (c) Deflection of MEMS Switch under Fully Actuated Conditions.

3.6.2 RF Design

In all RF switch designs, the actuation mechanism is important for its characterization. Any switch is assumed to be binary and digital in the sense that it can lie in one of only two possible actuation states. In the on state, the switch is configured to connect to the input port of a system to the output port, whereas in the off state, the switch is configured to disconnect the ports. The number of poles is defined as the number of input terminals or input ports to the switch, and the number of throws is the number of output terminals or output ports. The possible RF measurements to be done on any switch are: (a) insertion loss in the on state; (b) isolation in the off state; and (c) return loss in both states.

3.6.2.1 Transmission lines

Vardhan (2003) delectated that if we consider a transmission line of characteristic impedance Z_0 feeding a different line of impedance Z_1. It is assumed that there is no reflection from the load, the

input impedance seen by the feed line Z_1, so that the reflection coefficient Γ, which is defined as the amplitude of the reflected voltage wave normalized to the amplitude of the incident voltage wave, is

$$\Gamma = \frac{V_0^+}{V_0^-} = \frac{Z_1 - Z_0}{Z_1 + Z_0} \quad (3.1)$$

However, it can be seen that not all the incident wave is reflected: some of it is transmitted to the output port with voltage amplitude given by the transmission coefficient, T .The transmission coefficient can be written as

$$T = 1 + \Gamma = \frac{V_0^+}{V_0^-} = \frac{Z_1 - Z_0}{Z_1 + Z_0} = \frac{2Z_1}{Z_1 + Z_0} \quad (3.2)$$

The equations proposed by Vardhan (2003) depicted transmission coefficient between two points in a circuit is often expressed in decibels as the insertion loss, IL:

$$IL = -20 \log |T| \text{ dB} \quad (3.3)$$

When load is mismatched in a transmission line, not all the available power is delivered to the load. This loss is called return loss (RL) and is defined (in dB) as

$$RL = -20 \log |\Gamma| \text{ dB (3.48)} \quad (3.4)$$

so that matched load (Γ = 0) has a return loss of ∞ dB (no reflected power) while a total reflection (Γ = 1) has a return loss of 0 dB (all incident power is reflected). As |Γ | increases, the ratio of voltage amplitudes V_{max} and V_{min} also changes and its ratio also increases. The standing wave ratio (SWR) is a measure of mismatch of a line and is defined as

$$SWR = \frac{V_{MAX}}{V_{MIN}} = \frac{1+\Gamma}{1-\Gamma} \quad (3.5)$$

3.6.2.2 Microwave considerations

The microwave parameters that should be optimized for any RF switch are the insertion loss, isolation, switching frequency and the return loss. The insertion loss is mainly due to the mismatch between the characteristic impedances of the line and the switch. The contact resistance and the beam metallization loss will also contribute to the insertion loss. Li (2014) described that one of the principal requirements of RF MEMS switch design is the design of a transmission line structure that has to be a circuit element in a microwave integrated circuit (MIC). The structure, which is a planar configuration, has the property that its characteristic impedance is determined by the dimensions in

a single plane. For example, the impedance of a transmission line on a microwave substrate can be controlled by the width of the line. The common structures of planar transmission lines are shown in Figure 3.5. The micro strip line is the most commonly used MIC transmission line because of its advantages such as small size, low cost, no cutoff frequency, and ease of active device.

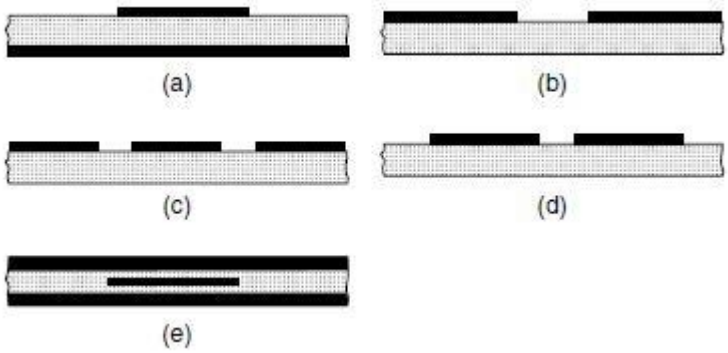

Figure 3.5 Different Configurations of Planar Transmission Lines Used in Microwave Integrated Circuits (Vardhan, 2003): (A) Micro Strip Line; (B) Slot Line; (c) Co-Planar Waveguide; (d) Co-Planar Strips; (e) Strip Line Configuration

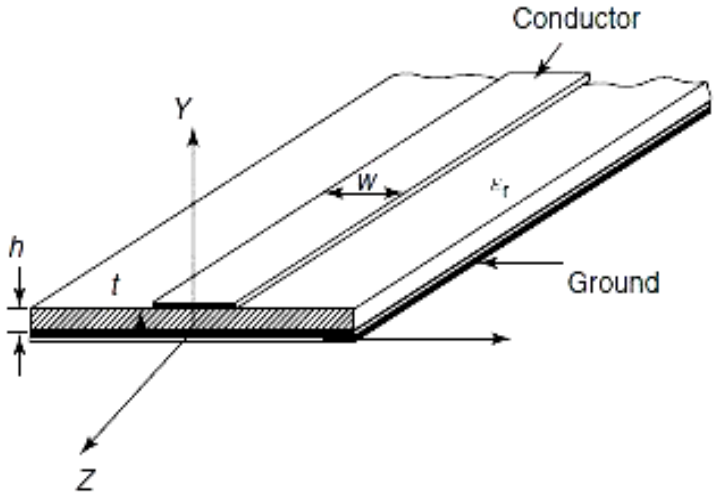

Figure 3.6: Depiction of Micro Strip Transmission Line

Monolithic circuits are MICs on a GaAs substrate with active and passive devices on the same chip. Compared with a rectangular waveguide, the disadvantages of micros trip lines are their higher loss, low power handling capability and greater temperature instability. Figure 3.6 shows the schematic diagram of the micro strip line. Vardhan (2003) explained that a thin conducting strip of width 'W' is etched on top of a grounded dielectric substrate with thickness h and relative permittivity ε_r. In general, two types of substrates are used: soft substrates and hard substrates. Soft substrates are flexible, cheap and are easy to fabricate. However, they have high thermal expansion coefficients.

Some typical soft substrates are RT Duroid 5870 (ε_r = 2.3), RT Duroid 5880 (ε_r = 2.2) and RT Duriod 6010 (ε_r = 10.5) (RT Duroid is the trademark of Rogers Corporation, Chandler, AZ). Hard substrates quartz (ε_r= 3.8), alumina (ε_r = 9.7), sapphire (ε_r = 11.7) and GaAs (ε_r = 12.3) have better reliability and lower thermal expansion coefficients but are more expensive and nonflexible as described by Huang (2012). The most important parameters in micro strip circuit design are width, height and the substrate dielectric constant ε_r.

3.6.2.3 Design of CPW (Coplanar Wave Guide)

CPW is the base of RF MEMS device which is fabricated to micromachining of either semiconductor or non-conducting materials on CPW have Two Grounds and one t-line which is probably same as the length of the MEMS Bridge, CPW is the Stationary Part where whole mechanism is set on it. Figure 3.7 shows the structure of CPW.

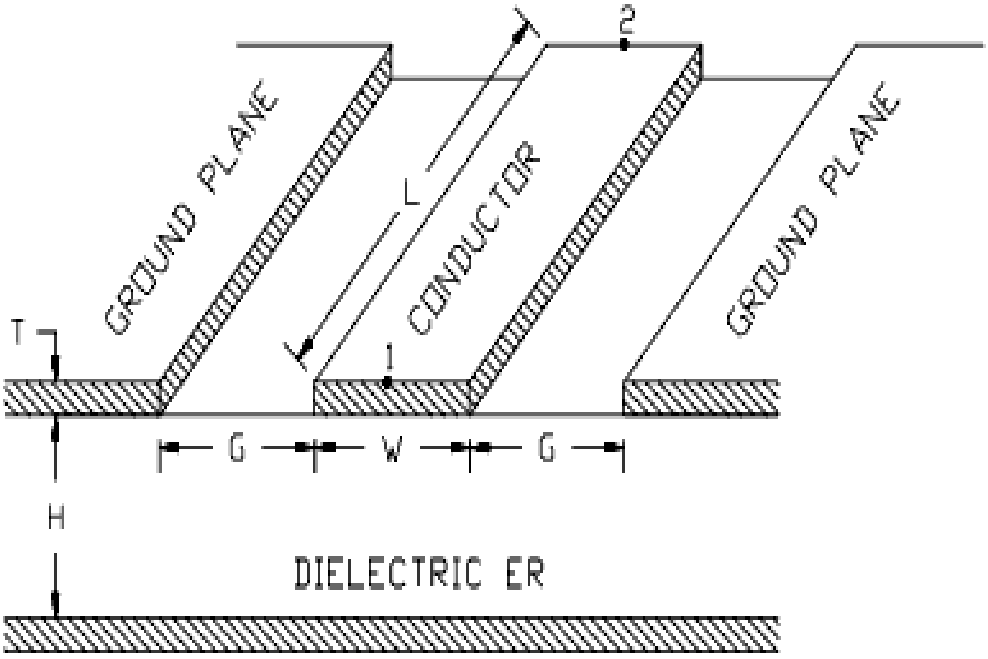

Figure 3.7: Depiction of Coplanar Wave Guide (CPW)

3.6.2.4 Design equations

A micro strip is a two-conductor transmission line that can be considered to have evolved conceptually from a two-wire transmission line. Micro strip lines differ considerably from other transmission lines. Compared with a strip line, the micro strip structure is open on the top. This configuration makes a micro strip very convenient for use in MICs where discrete lumped devices (active or passive) can be mounted in the circuit. Also because of the planar nature, impedance

matching as well as small tuning can be incorporated after the fabrication of the circuit. However, the presence of the dielectric–air interface modifies the mode of propagation in a micro strip and this open structure causes complications in analysis and design. Unlike strip line, where all fields are contained within a homogeneous dielectric medium, micro strip has most of its field lines in the dielectric region, concentrated between the strip conductor and the ground plane and some fraction in air above the substrate. Vardhan (2003) described that such a combination cannot support pure transverse electromagnetic (TEM) fields, since the phase velocity of TEM fields in air region would be c and that in the dielectric region would be $c/\sqrt{\varepsilon_r}$. In most of the practical applications, however, the dielectric substrate is electrically very thin ($h << \lambda$) and the fields are quasi-TEM. Thus a good approximation for the propagation constant, phase velocity and characteristic impedance can be obtained from the static or quasi-static approximations. The phase velocity and propagation constant can be expressed as prescribed by Vardhan (2003) as follows:

$$\upsilon_P = \frac{C}{\sqrt{\varepsilon_P}} \tag{3.6}$$

$$\beta = k_0\sqrt{\varepsilon_r} \tag{3.7}$$

where $\boldsymbol{\varepsilon_p}$ is the effective dielectric constant of the micro strip line. Since field lines are in the dielectric region as well as in air, the effective dielectric constant satisfies the relation and is dependent on the substrate thickens h and conductor width 'W'. Rebiez (2003) on the other had described that effective dielectric constant can be interpreted as the dielectric constant of a homogeneous medium that replaces the air and the dielectric regions of the micro strip. The effective dielectric constant of a micro strip line is given by

$$\varepsilon_e = \frac{\varepsilon_r+1}{2} + \frac{\varepsilon_r - 1}{2} \tag{3.8}$$

$$F\,(W/h) = \begin{cases} \left(1+\frac{12h}{w}\right)^{-1} + 0.04\left(1-\frac{w}{h}\right)^2, \text{for } \frac{w}{h} \le 1 \\ \left(1+\frac{12h}{w}\right)^{-1}, \text{for } \frac{w}{h} \ge 1 \end{cases} \tag{3.9}$$

The characteristic impedance of the micro strip line is given by

$$Z_0 = \begin{cases} \frac{60}{\sqrt{\varepsilon_r}}\ln\left(\frac{8h}{W}+\frac{W}{4h}\right), \text{ for } \frac{W}{h} \le 1 \\ 120\pi\left\{\sqrt{\varepsilon_r}\left[\frac{W}{h} + 1.393 + 0.667\ln\left(\frac{W}{h}\,1.444\right)\right]\right\}^{-1} \text{ for } \frac{W}{h} \ge 1 \end{cases} \tag{3.10}$$

For given characteristic impedance Z_2 and dielectric constant ε_r, the W/h ratio can be determined from,

$$\frac{W}{h} = \begin{cases} \frac{8e^{A}}{e^{2A}-2}, \text{for } \frac{W}{h} < 2 \\ \frac{2}{\pi}\{B - 1 - \ln(2B-1) + \frac{\varepsilon_r - 1}{2\varepsilon_r}\left(\ln(B-1) + .39 + \frac{0.61}{\varepsilon_r}\right), \text{for } \frac{W}{h} \end{cases} \quad (3.11)$$

$$A = \frac{Z_0}{60}\left(\frac{\varepsilon_r+1}{2}\right)^{1/2} + \frac{\varepsilon_r - 1}{\varepsilon_r+1}\left(0.23 + \frac{0.11}{\varepsilon_r}\right) \quad (3.12)$$

and $B = \frac{377\pi}{2Z_0\sqrt{\varepsilon_r}}$

(3.13)

Vardhan (2003) refers mathematical equations that relate to the impedance value decreases when the strip to height ratio (W/h) of the substrate is increased because an increase in W (or a decrease in h) will increase the line capacitance. These expressions provide accuracy better than 1%. A more accurate expression for the characteristic impedance Z_0 of a micro strip for t = 0 and $\varepsilon_r = 1$ is given by (Gupta et al., 1996)

$$Z_0 = 60 \ln\left\{\frac{f(x)}{x} + \left[1 + \left(\frac{2}{x}\right)^2\right]^{1/2}\right\} \quad (3.14)$$

$$f(x) = 6 + (2\pi - 6)\exp\left[-\left(\frac{30.666}{x}\right)^{.7528}\right] \quad (3.15)$$

and x = W/h. The accuracy of this expression is better that 0.01% for $x \leq 1$ and 0.03 percent for $x \leq 1000$.

3.6.2.5 Power-handling capability

It is well known that, in general, the micro strip lines are suitable only for low-power applications. Although micro strip circuits are not well suited for high-power applications as, like waveguides of coaxial lines, they could possibly be used for several medium-powers applications. For example, a micro strip line on a 25-mm thick alumina substrate can handle a few kilowatts of power. The power-handling capacity of the micro strip circuit is limited by the heating because of the ohmic and dielectric losses and by dielectric breakdown. An increase in temperature due to dielectric as well as conductor losses limit the average power, while the breakdown between the strip conductor and ground plane limits its ability to handle peak power.

3.6.2.6 Micro strip losses

Rebiez (2003) described that the RF weakening in a miniaturized scale strip structure is created by two parts: conductor loss and dielectric loss. The magnetic loss segment will likewise be show for a magnetic substrate. For a conductor, the surface impedance Z_s (equivalent to R + jX) has a genuine part R (surface resistance every unit length), which is equivalent to the nonexistent part X. That is,

$$R = X = \omega L \quad (3.16)$$

Where L is the inductance every unit length. Rebiez (2003) described that the inductance L of the smaller scale strip structure can be communicated regarding the characteristic impedance for the smaller scale strip with the substrate supplanted via air and is given as

$$L = \frac{Z0air}{c} \tag{3.17}$$

where c is the speed of electromagnetic waves in free space. When in doubt it can be expressed that the thickness of the conductors ought to be greater than around four times the skin depth. It is watched that the conductor losses are lessened by around 9% when the conductor thickness is $\pi/2$ times the skin depth. The lessening constant for a smaller scale strip line because of dielectric loss can be composed as

$$\propto_d = 27.3 \frac{(\varepsilon_r)}{(\sqrt{\varepsilon_e})} \frac{\varepsilon_e - 1}{\varepsilon_r - 1} \frac{tan\delta}{\lambda_0} \tag{3.18}$$

Vardhan (2003) proposed that where (tan δ) is the loss digression of the dielectric substrate. For a small scale strip line on alumina substrate the dielectric loss αd is irrelevant contrasted and aggregate loss α. Notwithstanding, for small scale strip lines on semiconductor substrates, for example, silicon, the loss variable is overwhelming. A small scale strip line on a silicon substrate with dielectric constant ε_r = 11.7 and a resistivity of 103 cm has a dielectric loss of the request of 0.36 dB cm^{-1}, while the transmitter loss is around 0.19 dB cm^{-1}.

3.7 DESIGN PROCEDURE ON COMSOL 5.0 MULTIPHYSICS SOFTWARE

COMSOL Multiphysics is a finite element analysis, solver and Simulation software / FEA Software package for various physics and engineering applications, especially coupled phenomena, or multiphysics. COMSOL Multiphysics also offers an extensive interface to MATLAB and its toolboxes for a large variety of programming, preprocessing and post processing possibilities. The packages are cross-platform (Windows, Mac, Linux). Furthermore, ANSYS dimensional parameter is in metrics, otherwise COMSOL can perform in metrics and micrometers. COMSOL is specially framed with MEMS module which is not available in ANSYS and CATIA. Also, in addition to conventional physics-based user interfaces, COMSOL Multiphysics also allows for entering coupled systems of partial differential equations (PDEs). The PDEs can be entered directly or using the so-called weak form (see finite element method for a description of weak formulation). An early version (before 2005) of COMSOL Multiphysics was called FEMLAB. First, make a Coplanar Waveguide on Console window and adding the material with the help of material library which is given to COMSOL library. Step by step simulation procedure is described as follows,

i) Defining Physics.

Start by selecting the space dimension for your model component: 3D, 2D Axisymmetric, 2D, 1D Axisymmetric, or 0D.

ii) Defining Geometry.

Geometry decides whether modal in mm, μm and m etc. it provides tools to make a proper design itself and also an option to import geometry through the other convectional Software.

iii) Defining Material.

It has some preloaded material tree where all material is present also their property, material tree helps to find MEMS Material and make less effort to define their properties.

iv) Setting Up Physics.

In here when the geometry and materials are defined, the boundary conditions are going to be set like, fixed constrain, boundary load etc.

v) Meshing.

The mesh settings determine the resolution of the finite element mesh used to discretize the model. The finite element method divides the model into small elements of geometrically simple shapes, in this case tetrahedrons. COMSOL (2012) each tetrahedron, a set of polynomial functions is used to approximate the structural displacement field—how much the object deforms in each of the three coordinate directions.

vi) Simulation and Study.

At the beginning of setting up the Physics it selected a Stationary study, which implies that COMSOL will use a stationary solver. For this to be applicable, the assumption is that the load, deformation, and stress do not vary in time. The default solver settings will be good for this simulation if your computer has more than 6 GB of in-core memory (RAM). If you should run out of memory so more complex the design more memory will be used. The whole process of study is depends upon in Meshing either fine or coarse.

Figure 3.8 depicts the process simulation process gradient with modeling of feasible modified design. Figure 3.9 relates to calculation of stress gradients in terms of von Mises and contact force. The strip design will have the database of COMSOL.

3.8 SYSTEM SIMULATION WORK

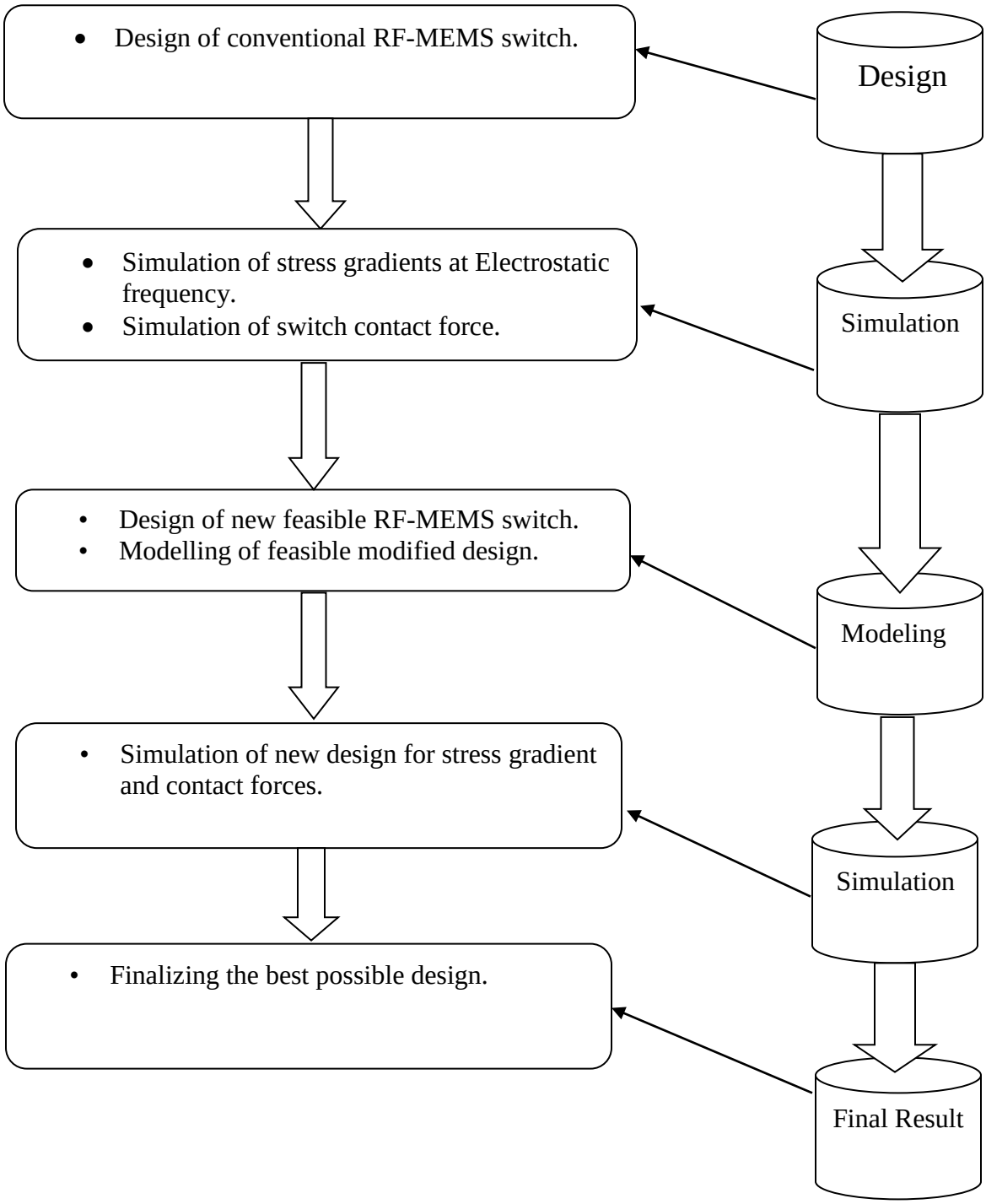

Figure 3.8: Simulation Process Algorithm

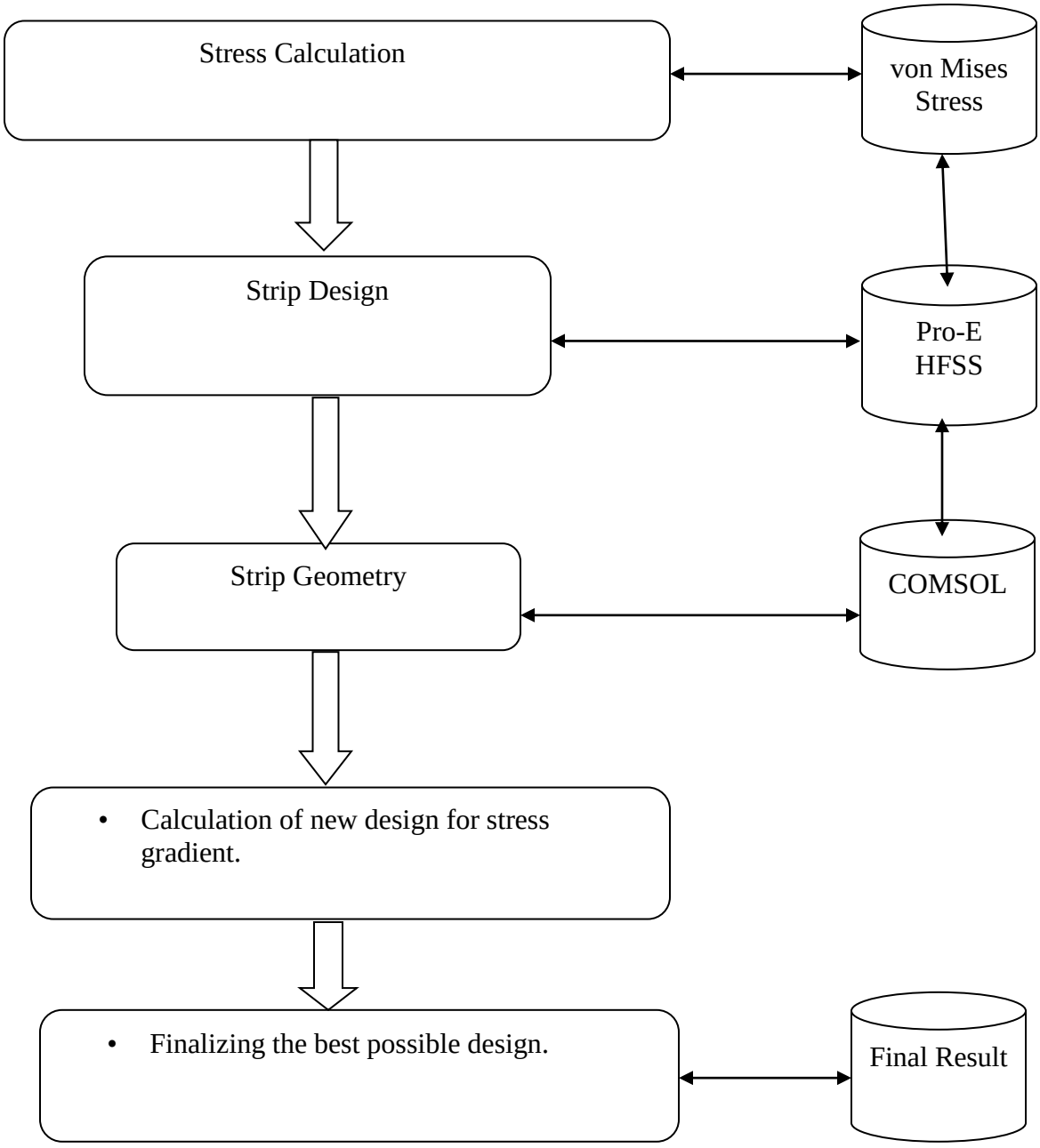

Figure 3.9: Design of Calculation and Simulation Algorithm

CHAPTER 4: RESULTS AND DISCUSSION

This chapter consists of the steps taken for the designing, modeling, simulations and analysis of the contact membrane of the RF MEMS switch. The designing and modeling is performed on Pro-e designing software platform and all the simulations and analysis process are performed with the help of COMSOL 5.0. The system indicators are RF MEMS switch; cantilever beam; membrane; flexures; signal contact surface; stress gradients; electrostatic actuation; beam displacement; total strain energy and reliability.

4.1 GEOMETRY OF RF MEMBRANE

Definition of geometry on the analysis software is provided in which the dimensional configurations are defined as shown in Figure 4.1.

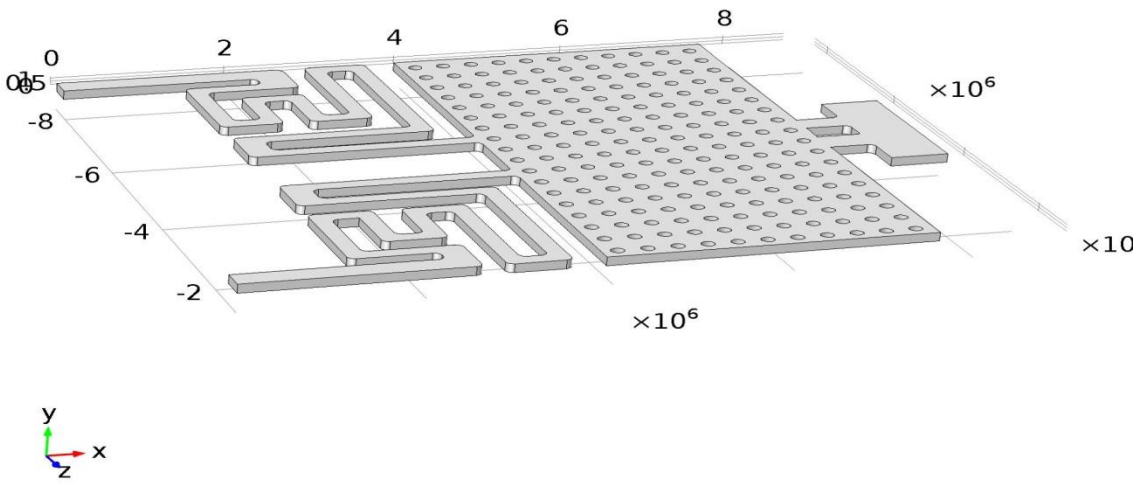

Figure 4.1: Geometry of the Actuating Membrane (COMSOL).

Figure 4.1 depicts the actuating membrane in which a hybrid of Crab Leg and Serpentine flexures and the beam edges are provided with fillets in order to avoid higher stress concentrations whose applications and benefits are obtained in results. The beam distance that is the combined length of crab leg and serpentine flexure is taken to be 154 microns. The fillet radius is provided to be 3 microns as per the feasibility of design. The membrane width is taken to be145 microns and the contact metal strip distance from membrane from edge to edge is taken to be 46 microns. The radius

of perforation holes is taken to be 3microns and the pitch distance between them is 6 microns. The contact membrane is provided with perforations for lowering the air resistance hence providing smooth operations. The tip where contact metal is located is provided with a pyramid line contact surface such that the circuit is completed just with mere finite point contacts reducing the contact area and hence the reactivity in case of high temperature applications. Table 4.1 addresses the geometrical values taken by the COMSOL software in order to generate the pathway for the analysis. It describes the number of entities taken for assignment of different commands and boundaries for propagations of analysis procedure.

Table 4.1: Geometry Statistics

Property	**Value**
Space dimension	3
Number of domains	1
Number of boundaries	541
Number of edges	1617
Number of vertices	1078

4.2 MATERIAL OF RF MEMBRANE

The material taken for layer is Borosilicate as it is synthetically safe, has a low thermal expansion coefficient and can be utilized at moderately high temperatures. It is accessible in numerous structures and sizes and as machined or hot shaped parts. It is effortlessly available and is exceptionally financially savvy for assembling. Borosilicate is generally utilized as a part of synthetic and building applications. Borosilicate offers a higher greatest utilization temperature and better thermal stun properties. Borosilicate is greatly artificially safe, has a low thermal expansion coefficient. It is accessible in numerous sizes and structures, for example, bar, tube, plate and as machined or hot shaped parts. Tables 4.2, 4.3 and 4.4 show the material properties, basic settings for the material predefined properties in software and values of Young’s modulus and Poisson’s ratio for the borosilicate glass.

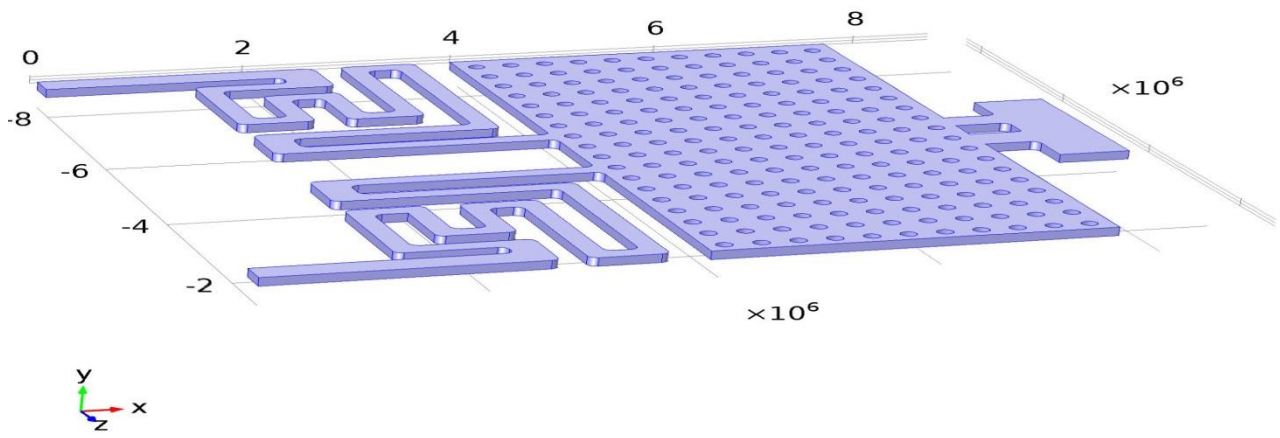

Figure 4.2: Borosilicate Assigned For Membrane

Table 4.2: Material Parameters

Name	Value	Unit
Density	2230[kg/m^3]	kg/m^3
Young's modulus	63e9[Pa]	Pa
Poisson's ratio	0.20	1

Table 4.3: Borosilicate Physical Parameters

Description	Value
Dielectric Constant	4.6
Coefficient of thermal expansion	3.3 x 10^{-6}/Celcius
Heat capacity at constant pressure	754[J/(kg*K)]
Relative permittivity	4.8
Density	2230[kg/m^3]
Thermal conductivity	1.13W/(m*K)

Table 4.4: Borosilicate Properties of Young's Modulus and Poisson's Ratio

Description	Value
Young's modulus	63e9[Pa]
Poisson's ratio	0.20

4.3 FIXED CONSTRAINTS OF RF MEMBRANE

For the initial cantilever actions the beam is assigned with fixed boundaries from where the beam will not displace and the loads are not applicable so that the cantilever action is obtained while the electrostatic actuation is applied on the contact surface. Figure 4.2 and Figure 4.3 show the fixed constraints for the designed actuating membrane.

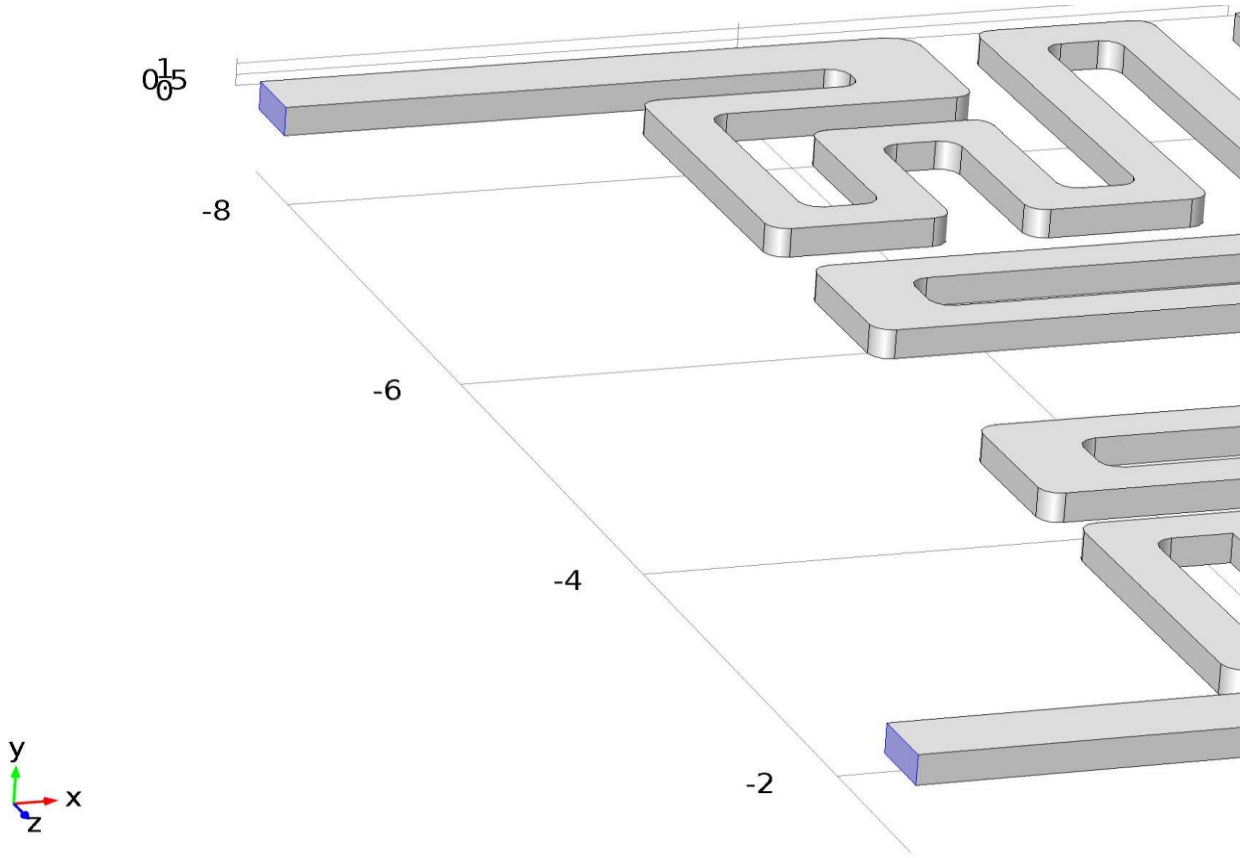

Figure 4.3: Fixed Constraints Applied on the Edge of the Beams

4.4 MESHING OF THE RF MEMBRANE BEAM

The meshing of beam is taken after the boundary constraints are provided with the electro mechanics constraints having defined with the electron voltage for electrostatic actuation, bending of beam by electromagnetic forces and the contact of the beam by the ground planes. The mesh constraints are taken by free tetrahedral for proper analysis of tetrahedral finite element boundaries. For the convenience of workstation, the mesh size is taken to be for a fine size instead of extremely fine in order to obtain the results.

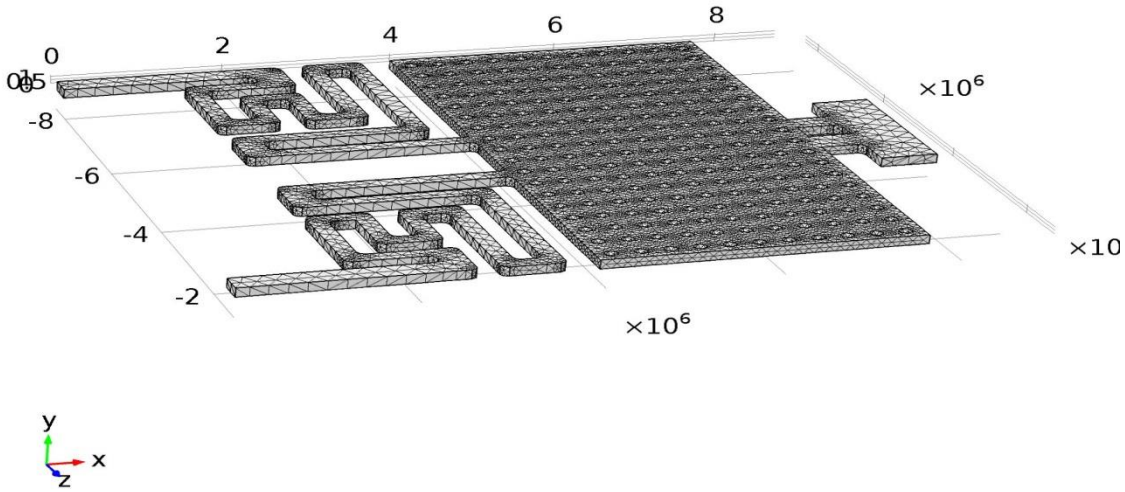

Figure 4.4: Free Tetrahedral Meshing of Actuating Membrane

Table 4.5: Meshing Size Settings

Name	Value
Maximum element size	701000
Minimum element size	87600
Curvature factor	0.5
Resolution of narrow regions	0.6
Maximum element growth rate	1.45
Predefined size	Fine

4.5 CANTILEVER BEAM DESIGNING AND SIMULATION

The finalized design is subjected to electrostatic actuation; bending of membrane; von Mises stress computation; parallel plate capacitance and electric potential.

4.5.1 Coplanar Wave Guide

The proposed RF MEMS switch comprises of a coplanar wave guide (CPW) line for the RF signal transmission, and anodes for electrostatic activation on Sapphire substrate, as indicated in Figure 4.5. The CPW line comprises of a contact surface line, a draw down cathode moored at the ground line, the contact layer, dielectric and the contact metal at the furthest end of the twisting film. The film lies on the ground plane where it is anchored as indicated in the Figure 4.5.

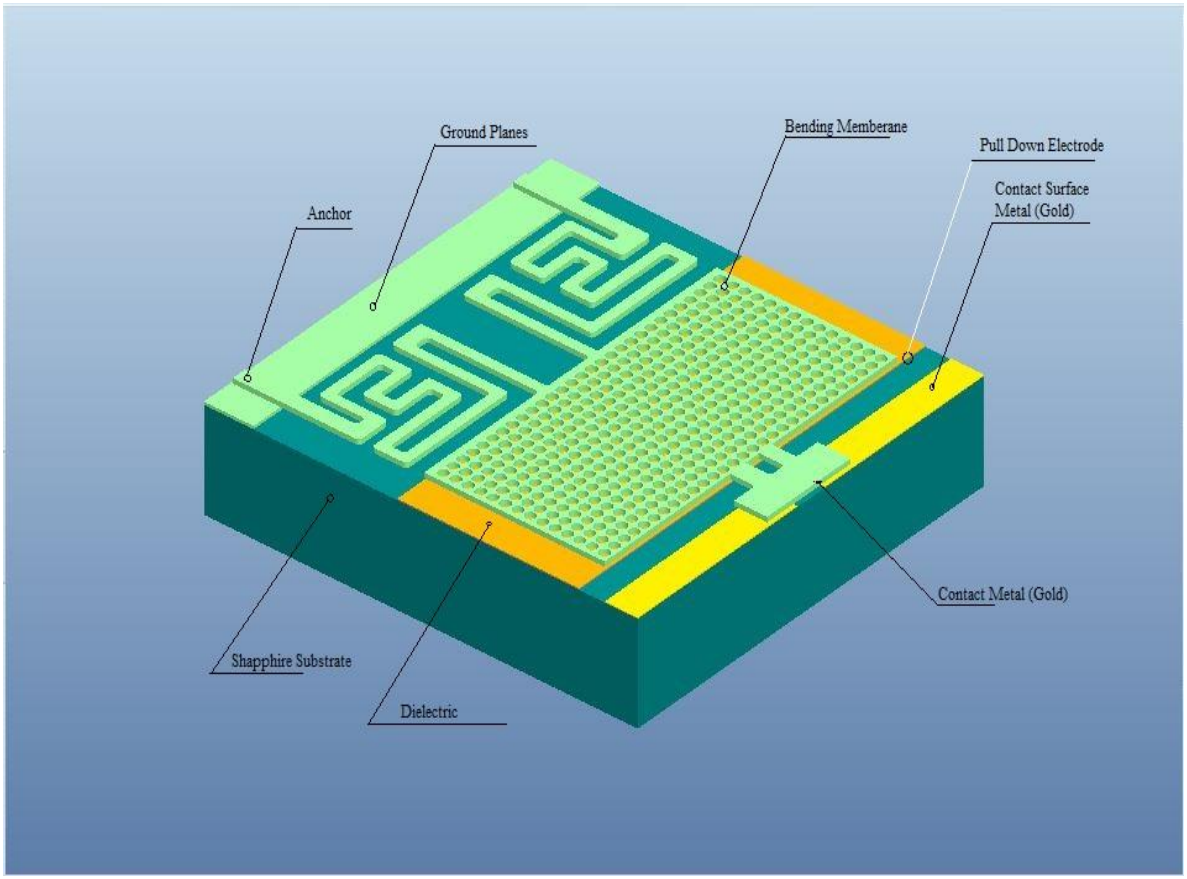

Figure 4.5: Coplanar Waveguide for Cantilever Beam Switch Mechanism

The membrane is provided with crab leg and serpentine flexures, which bring about low values for the spring constant and smoother moves of the layer. Figure 4.5 shows individualized, clarified and checked segments of the switch, to give an unmistakable comprehension of the outline. The draw down anode underneath the contact surface is arranged in the same plane as the CPW which is secured with a dielectric layer. The contact metal altered underneath the most distant tip of the layer

furnishes contact surface with the open signal line, when the switch is activated. The Flexures are altered to the ground plane. The fundamental working guideline of the proposed switch is taking into account the bending movement of a non-consistently stacked beam. The portable part rests far from the beginning, is activated through draw down electrodes, bringing about the lever sort stressed movement. At the point when no incitation voltage is connected to the draw down terminal, the beam backpedals to "rest-state". At the point when incitation voltage is connected to the draw down anode secured with dielectric, the switch is actuated, and it touches down on the transmission line, and shuts the open circuit of contact metal circuit transmission line. This methods is termed as the "down-state" or "ON-state", when incitation voltage is not running over the draw down electrode, the beam moves back to its unique spot and consequently the contact metal moves away above from the RF signal or transmission line, which is at the introductory crevice between the two at the rest-state. This is the "OFF-state", and results in detachment. Consequently, this configuration proposes a switch that is stiction-denied and has an extremely huge segregation. As a result of the ground thickness of the layer, there is an exceptionally critical hole between the contact metal and RF transmission line is kept up without the impacts of bending or stiction, making it conceivable to utilize the switch at low voltage.

4.5.2 Electric Potential

An electrostatic power brought on by a connected potential contrast between the electrode and film twists the beam toward the grounded plane underneath it. To process the electrostatic power, the electric field in the encompassing air for the film beginning beam is ascertained. The model considers a layer of air 20 μm thick both above and to the sides of the beam, and the air hole between the base of the beam and the grounded layer is at first 2 μm. As the beam twists, the geometry of the air hole changes persistently, bringing about an adjustment in the electric field between the electrodes. The coupled physics is taken care of consequently by the Electro mechanics interface. The electrostatic field noticeable all around and in the beam is represented by Poisson's mathematical statement, where subsidiaries are brought as for the spatial directions. This model shows the electric potential and its sub branches on a lattice which is moving concerning the spatial edge.

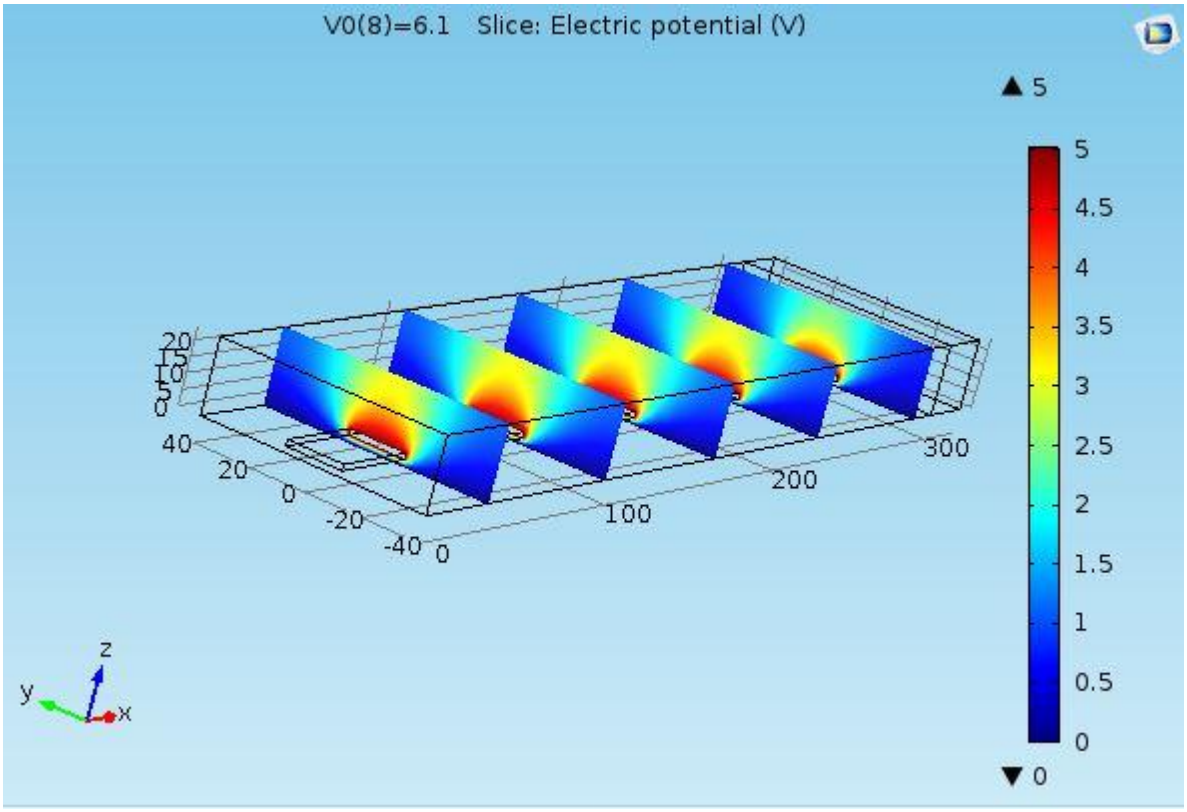

Figure 4.6: Electric Potential on the Actuating Beam

In Figure 4.6, fundamental changes are dealt with by the Electro mechanics interface, which additionally contains smoothing comparisons representing the movement of the lattice noticeable all around area. The cantilever joins with a voltage terminal with a predetermined predisposition potential, V_{in}. The base of the load is grounded, while other boundaries are electrically protected. The terminal limit condition naturally registers the capacitance of the framework. The power thickness that follows up on the electrode of the beam results from Maxwell's push tensor which is computed by the Multiphysics Platform. Figure 4.7 demonstrates the electric power which is constantly situated along the ordinary of the limit. Navier's mathematical statements, which represent the distortion of a solid, are all the more helpfully written in a direction framework that takes after and distorts with the material. For this situation, these reference or material directions are indistinguishable to the genuine lattice coordinates.

4.5.3 Beam Actuations under Electrostatic Forces

There is sure feedback between the electrostatic forces and the deformation of the cantilever beam. The forces twist the beam and consequently decrease the hole to the grounded substrate. At a certain voltage, the electrostatic forces overcome the actuation forces and the framework gets to be unstable, and the whole gap breakdowns. This basic voltage is known as the draw in voltage. At

connected voltages lower than the draw in voltage, the beam stays in a harmony position where the actuation forces adjust the electrostatic forces.

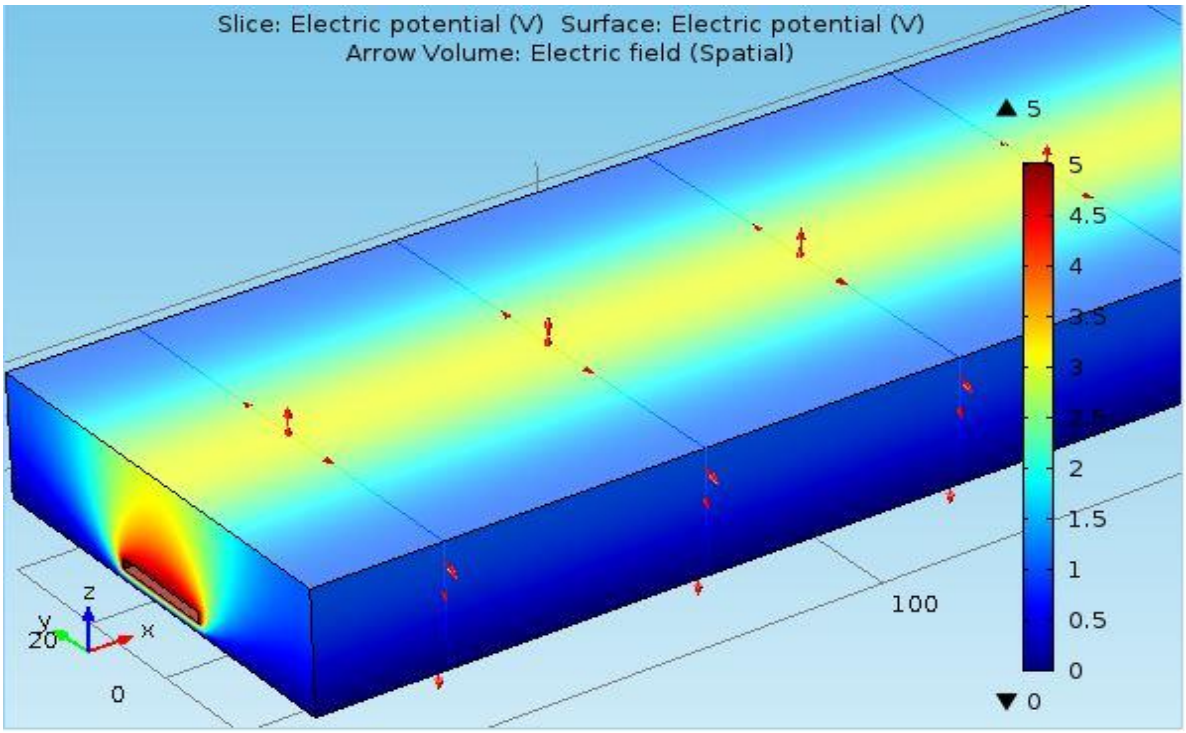

Figure 4.7: Electric Field Arrows Shown on the Beam Surface

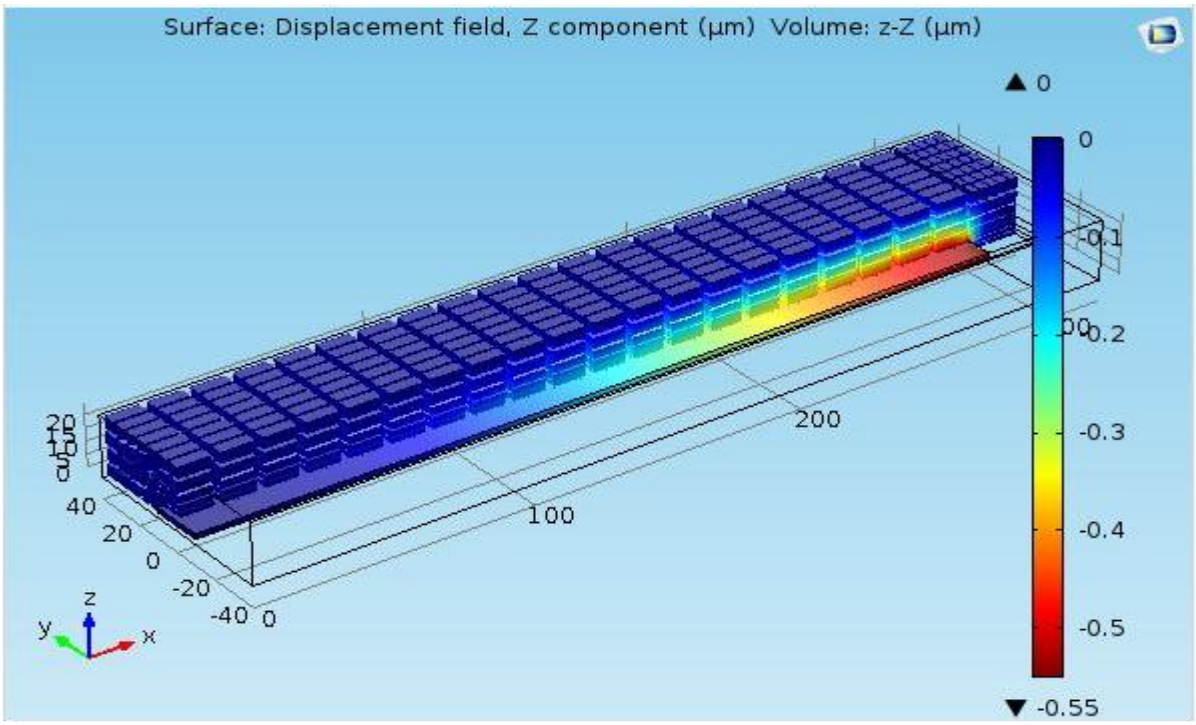

Figure 4.8: Flexure Bending Under the Effect of Electrostatic Forces

Figure 4.8 shows the beam displacement and the corresponding displacement of the mesh surrounding.

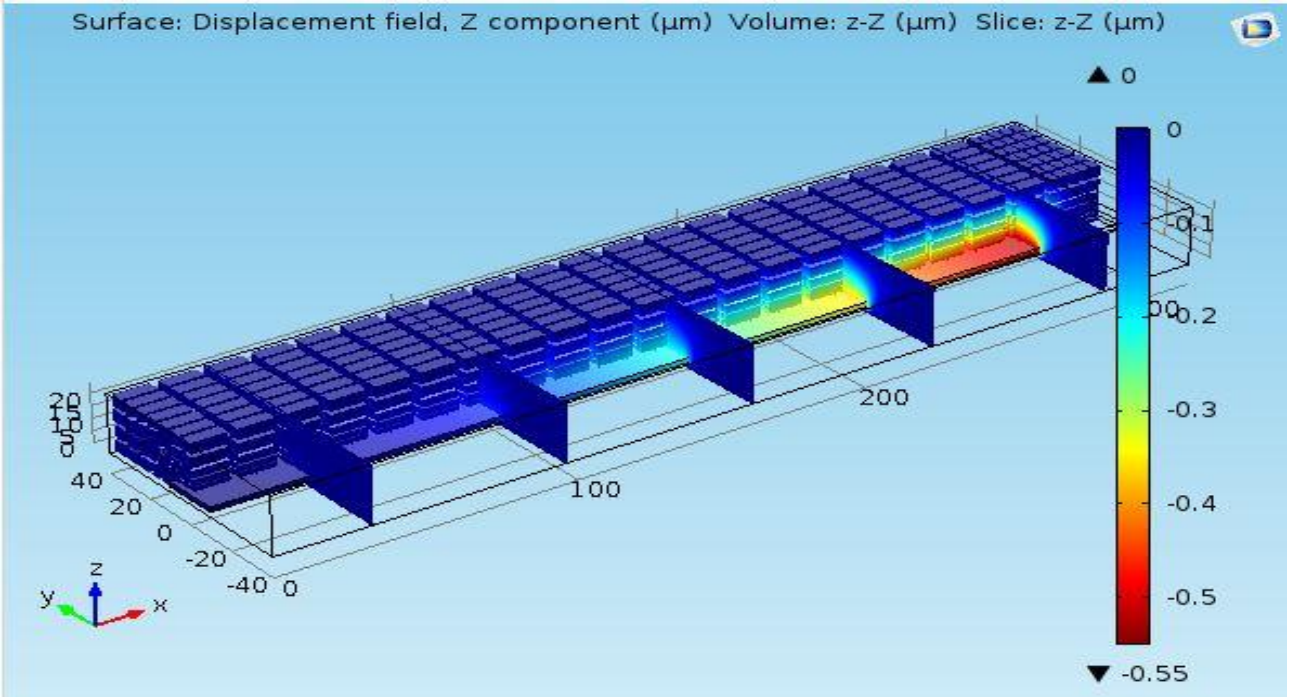

Figure 4.9: Depiction of Shape of Cantilever's Deflection for Each Applied Voltage

In Figure 4.9, the shape of the cantilever's deflection is illustrated for each applied voltage, by plotting the z-displacement of the underside of the beam at the symmetry boundary. The tip deflection as a function of applied voltage is shown in Figure 4.9. Note that for applied voltages higher than the pull-in voltage, the solution will not converge because no stable stationary solution exists. This situation occurs if an applied voltage of 6.2 V is tried. The pull-in voltage is therefore between 6.1 V and 6.2 V.

4.6 SIMULATION AND VALIDATION OF RF MEMS DEVICE

In Figure 4.10, the minimum von Mises stress obtained from the whole membrane analysis is computed out to be 6.66 x 10^5 µN/m^2 for maximum permissibility i.e. the maximum amount of the stress gradient that is produced in the beam where the pull down forces are applicable. The maximum stress gradient produced in the beam flexures obtained from bending of the beam is found out to be 200 µN/m^2 which shows the effectiveness of the hybrid design of beam with crab leg and serpentine flexures. The previously designed MEMS cantilever switch by LI (2014) showed the computational values of 4000 µN/m^2-5400 µN/m^2 which shows us the effectiveness of new design

compared to the old designs. This is the finalized results for the membrane for reduced stress gradient.

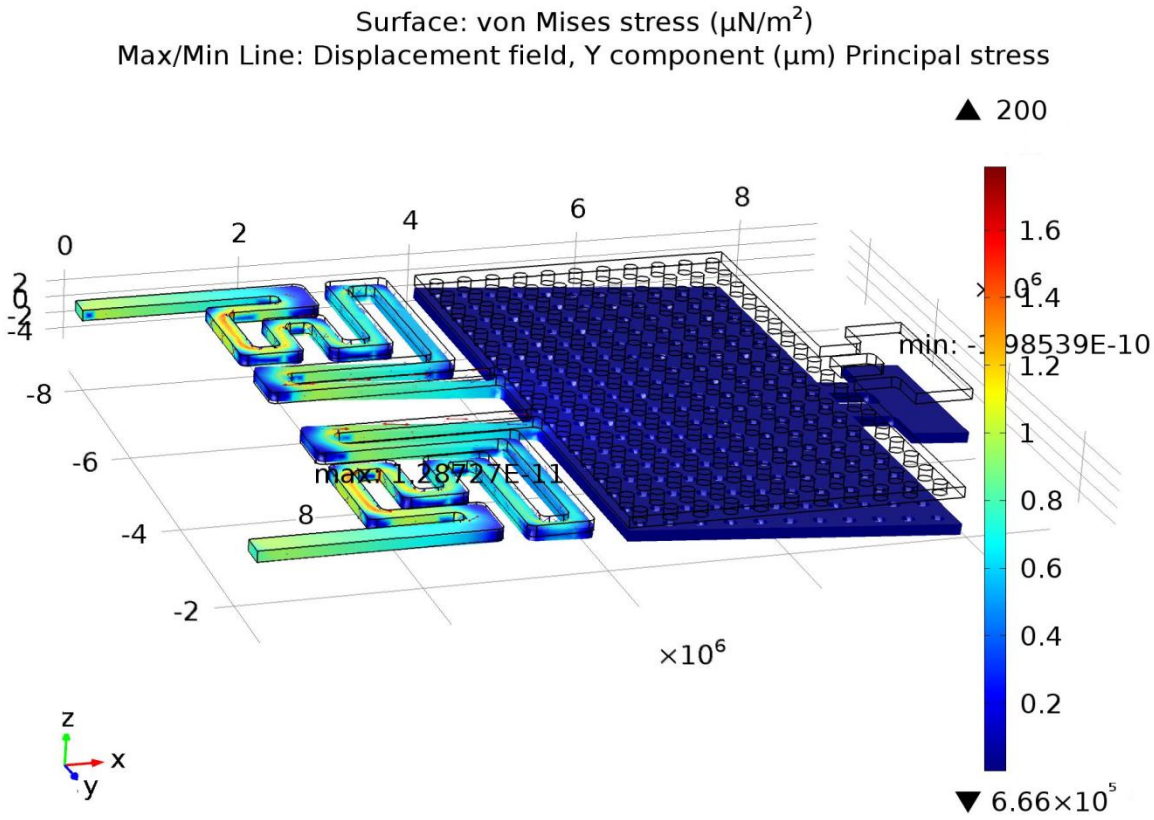

Figure 4.10: von Mises stress (μN/m^2) Max/Min Line: Displacement Field, Y Component (μm) Principal Stress

The displacement field is shown in the Figure 4.11 which shows the step by step bending of beam along with applied voltage of the proposed structure. The negative sign for the z displacements is because of the plane geometry along positive z-axis. The elastic strain energy produced in the beam is computed as per shown in Figure 4.12. The graphical representation of the provided graph shows that with every applied voltages and the elastic strain energy increases in very finite proportions for the best possible retraction of the bending beam to its original position hence causing the beam to regain its original position and also low elastic strain energy values provides the information that the lower actuation voltages are required for the movement of beam towards the pull down electrode. Figure 4.13 shows the DC C-V curve predicted for the cantilever beam. To some extent, this is consistent with the behavior of an ideal parallel plate capacitor, whose capacitance increases while the distance between the plates starts to diminish.

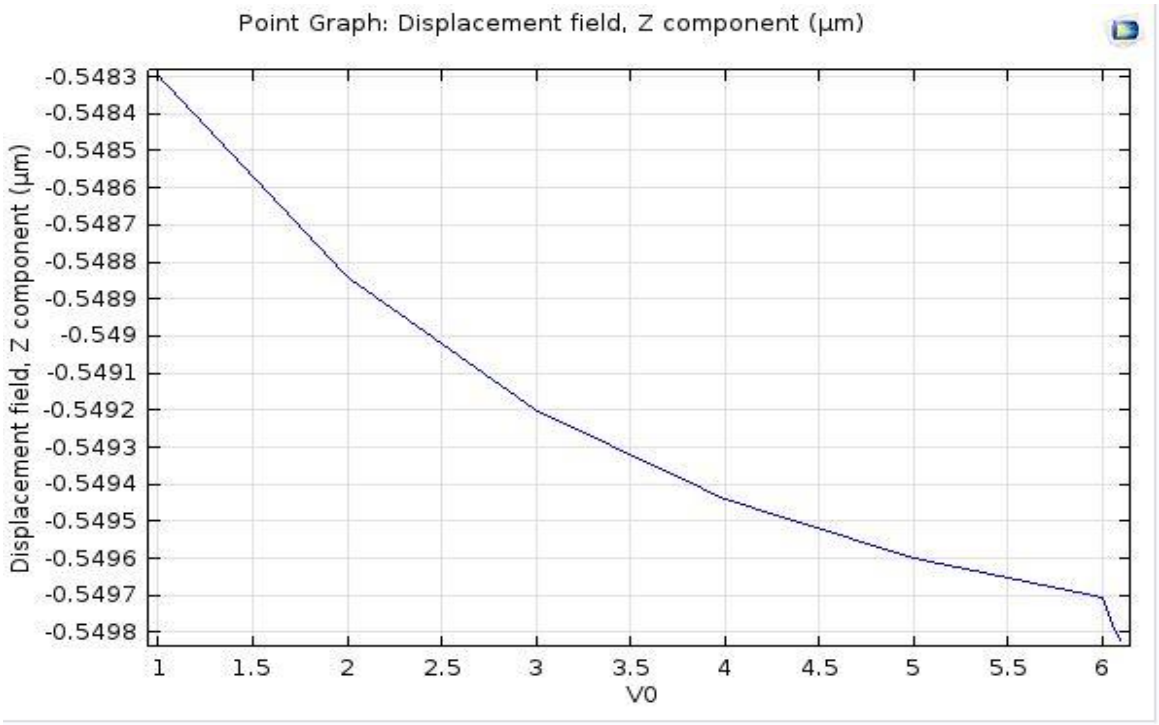

Figure 4.11: Displacement Field Along z-axis with Applied Voltage Step by Step

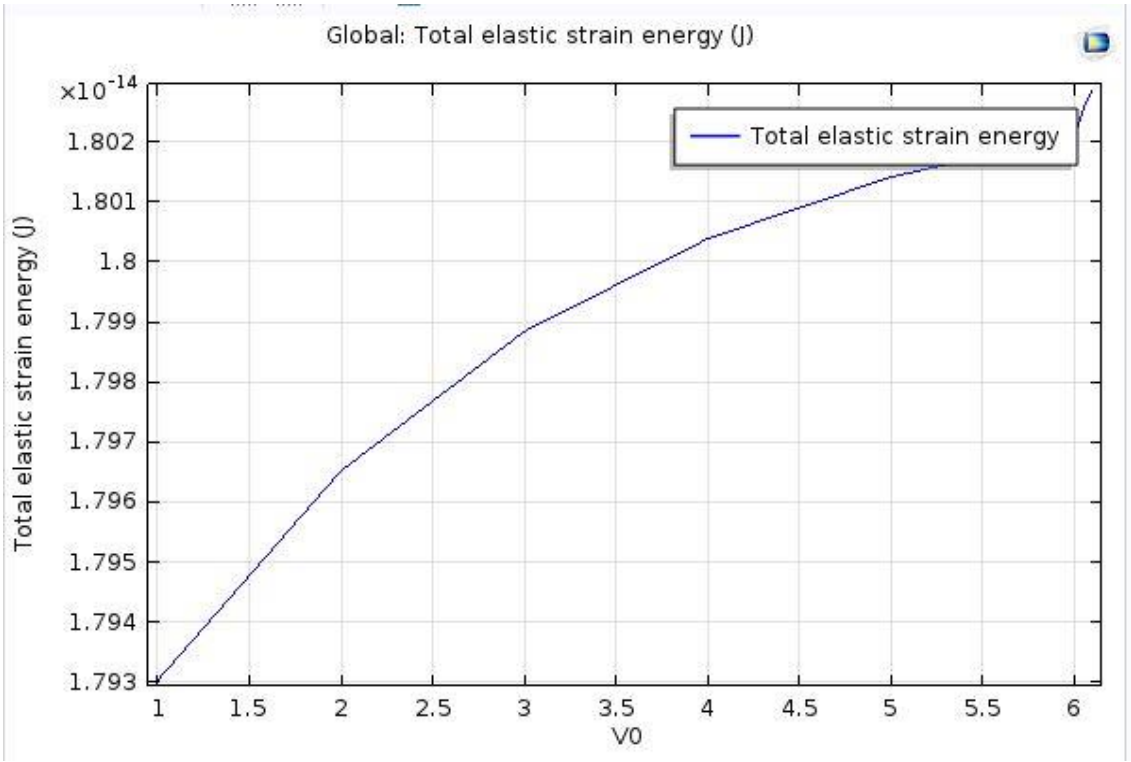

Figure 4.12: Voltage Applied Vs. Total Elastic Strain Energy

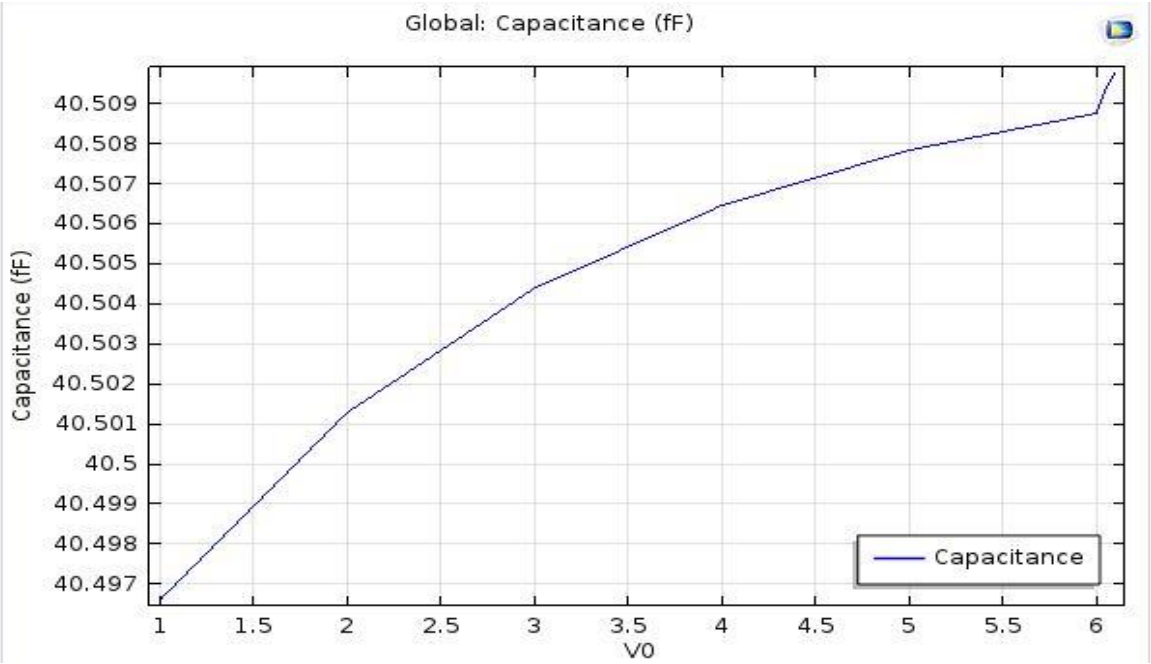

Figure 4.13: Beam Capacitance Along with Pull-down Electrode

But this effect does not account for all the change in capacitance observed. Mostly, the majority of it is because of the steady softening of the coupled electromechanical framework. This impact prompts a bigger auxiliary reaction for a given voltage increase at higher predisposition, which thus implies that more charge must be added to hold the voltage distinction between the electrodes. After the compilation of various forces and actuation mechanisms being implemented on the proposed design the actuation voltage is found out to be ranging between 6 – 6.2 voltage, the von Mises stress was found to be 200 $\mu N/m^2$, while the maximum applicable load was 6.66 x 10^5 $\mu N/m^2$ which promises the better reliability of the switch. Simulation test is performed on Multi User MEMS Process (MUMPS) technology in COMSOL 5.0 software Platform which validates the above results because of its minimum tolerance of error.

CHAPTER 5: CONCLUSION AND FUTURE SCOPE OF WORK

5.1 CONCLUSION

RF MEMS switches offer significant benefits and may be incorporated into many communication devices. Understanding switch behavior and characteristics is important for designers. Basic switch modeling has been completed. The novel configuration for beams with hybrid switch configuration are studied and analyzed. Its scientific model is likewise inferred to encourage correlations. At that point, its FEM is made and reenacted in COMSOL® to demonstrate its better static and transient execution over the others. Despite the fact that the moving beams in this configuration are of proportionate size and torsional solidness, changes to the beams can be made to meet a particular application. Besides, this idea can be effectively reached out to make a less complex outline with crossover flexures and utilization of point contacts over the contact ranges basically at the transmission line. The use of fillets at the edges of flexures helps to reduce the stress gradients by a great extent and hence must be applied for meanders designs to help the reduction of stresses in previously designed RF MEMS switches. In this dissertation, the design, and testing of RF MEMS contact switch with hybrid flexures was presented. Analytic stress gradient models were developed and resulted in predictions that agreed with measured graphical values. Overall, the results show increased lifetimes at the expense of a small increase of geometrical values for RF MEMS devices.

5.2 RECOMMENDATIONS

1. The system would suggest that the model to be designed must be free of sharp edges.
2. It is recommended that the hybrid mixture of crab leg and serpentine beam flexure are to be used for the better availability of spring constant.
3. It is recommended the pull down member of the switch should be designed as small as possible in proportion to the beam structures of flexures.
4. The present research work would suggest the implementation of analytical software like COMSOL and ANSYS modules for the calculation of stress gradients and elastic strain energy.
5. The present research work would optimize the designing criteria for the future MEMS switches with a better spring constants for cantilevered or capacitive switches.

5.3 FUTURE SCOPE OF WORK

The difference between the designs of different switches is quite high which give a clear illustration of different models for each switch that what kind of geometry change is applicable for best designing of product. It is observed that manufacturing suffer serious issues due to complexity of design.

- The future work includes a framing of a more easy to manufacture design of RF MEMS switches.
- The material for the beam structures are subject to change for better results and cheap manufacturing of switch.
- The development of user friendly interface for the analysis of the switches is needed for the upcoming researchers for quick access to the proposed design feasibility.
- Number of different designing software can be used for better finish results for the newly designed switches.
- It is a vast number of researches needed to be done for the betterment of substrate as currently few materials for substrate are available for the ground basis of MEMS devices.

REFERENCES

1. Basu, J. and Bhattacharyya, T. K. (2012), "Microelectromechanical System Cantilever-Based Frequency Doubles", Journal of Intelligent Material Systems and Structures, Vol. 42, 2, pp. 953-959.
2. Bhushan, B. (2003), "Adhesion and Stiction: Mechanisms, Measurement Techniques, and Methods for Reduction", Journal of Vascular Science and Technology, Vol. 21, 2, pp. 2262–2296.
3. Bhushan, B., Kasai, T., Kulik, G., Barbieri, L. and Hoffmann, P. (2005), "AFM Study of Per Fluoro Alkyls Lane and Alkyls Lane Self-Assembled Monolayers for Anti-Stiction in MEMS", Journal of Ultra microscopy, Vol. 105, 1, pp. 176–188.
4. Bhushan, B. (2007), "Nano Tribology and Nano Mechanics of MEMS and BioMEMS/Bio Materials and Devices", Proceedings of Microelectronics Engineering held at Ohio State University, Columbus, U.S., pp. 387-412.
5. DeGroot, W.A, Webster, JR., Felnhofer, D. and Gusev, EP. (2009), "Review of Device and Reliability Physics of Dielectrics in Electrostatically Driven MEMS Devices", Journal IEEE Trans Device Mater Reliability, Vol. 9, 3, pp. 190–202.
6. Fonseca, D. and Sequera. M. (2011), "MEMS Reliability and Failure Mechanisms", International Journal of Quality Statistics Reliability, Vol. 11, 2, pp. 1–7.
7. Holmberg, K, Matthews, A, and Ronkainen, H. (1998), "Coatings Tribology Contact Mechanisms and Surface Design", Tribological International Journal of Science and Technology, Vol. 31, 2, pp.107–120.
8. Huang, Y., Vasan, A.S., Doraiswami, R., Osterman, M. and Pecht, M. (2012), "MEMS Reliability Review", Journal of IEEE Trans Device Mater Reliability, Vol. 12, 2, pp. 482–493.
9. Huston, H. and Clarke, C. (1992), "Reliability Defect Detection and Screening During Processing: Theory and Implementation", Proceedings of International Reliability Physics Symp held at Fishkill, NY, USA, pp. 268-275.
10. Isono, Y. (2004), "Micro/Nano Materials Testing for Reliability Design of MEMS/Fourth International Symposium on Micro Nano Mechatronics for Information-Based Society", Proceedings of International Reliability Physics, Northwestern University, Japan, pp. 317-328.

11. Jau, T. and Wen. (2009), "MEMS Switches RF MEMS Switches: High- Frequency Performance and Hot-Switching Reliability", Journal of High Frequency Electronics, Vol. 23, 2, pp. 32-38.
12. Jeng, S., Lu, J. and Wang, K. (2007), "A Review of Reliability Research on Nanotechnology", Journal of IEEE Trans Reliability, Vol. 56, 2, pp. 401–410.
13. Ke, C., Espinosa, H. (2006), "In Situ Electron Microscopy Electromechanical Characterization of a Bistable Device", Journal of Inter Science, Vol. 12, 3, pp. 1484– 1489.
14. Kuo, W. (2006), "Challenges Related to Reliability in Nano Electro", Journal of IEEE Transactions of Reliability, Vol. 55, 3, pp. 569–570.
15. Lee, J., Kim, M., Ko, S., Kang, H., Bae, W. and Kang, M. (2009), "3-Terminal Nano Electromechanical Switching Device In Insulating Liquid Media for Low Voltage Operation and Reliability Improvement", Journal of IEEE IEDM09, Vol. 23, 1, pp. 227–230.
16. Li, B., Zhang, Y. and Xaolin, Y., (2014), "Reliability Design about Release Holes in Beam of Fuse MEMS G-Switch", Sensors & Transducers, Vol. 178, 9, pp. 28-33.
17. Li, X. and Bhushan, B. (2003), "Fatigue Studies of Nano Scale Structures for MEMS/ Applications Using Nano Indentation Techniques", Journal of Surf Coat Technology, Vol. 163, 3, pp. 521–526.
18. Liu, J., Shi, Y., Li, P., Tang, J., Zhao, R. and Zhang, H. (2012), "Experimental Study on the Package of High-G Accelerometer", Journal of Sensors Actuators a Physics, Vol. 173, 2, pp. 1–8.
19. Loh, O., Wei, X., Ke, C., Sullivan, J. and Espinosa, H. (2011), "Robust Carbon Nanotube-Based Nano-Electromechanical Devices: Understanding and Eliminating Prevalent Failure Modes Using Alternative Electrode Materials", Journal of Interscience, Vol. 7,1 pp. 79–86.
20. Mustafa and Khan, H., (2009), "Microstructure Cantilever Beam for Current Measurement", South African Journal of Science, Vol. 105, 3, pp. 264-269.
21. Nunes, B., Serro, A., Oliveira, V., Montemor, M. Alves, E., and Saramago, B. (2011), "Ageing Effects on the Wettability Behavior of Laser Textured Silicon", Journal of Applied Surf Science , Vol. 257, 1, pp. 2604–2609.
22. Passi, V., Bhaskar, U., Pardoen, T., Södervall, U., Nilsson, B., and Peterson, G. (2012), "High-Throughput On-Chip Large Deformation of Silicon Nano Ribbons and Nanowires", Journal of Microelectromech System, Vol. 21, 1, pp. 822–829.

23. Saha, S., Hanke, U., Geir, U. and Trond. (2007), “Modeling of Spring Constant and Pull-Down Voltage Of Non-Uniform RF MEMS Cantilever”, Proceedings of the 2006 IEEE International Behavioral Modeling and Simulation Workshop (BMAS 2006), Trondium University, Norway, pp. 56-60.
24. Srikar, V. and Spearing, S. (2003), “A Critical Review of Micro Scale Mechanical Testing Methods Used in the Design of Microelectromechanical Systems”, Journal of Society of Experimental Mechatronics, Vol. 43, 1, pp. 238–247.
25. Tambe, N. and Bhushan, B. (2005), “Micro/Nano Tribological Characterization of PDMS and PMMA Used for Bio MEMS/ Applications”, Journal of Ultra Microscopy, Vol. 105, 2 pp. 238–247.
26. Tanner, D. (2000), “Reliability of Surface Micro Machined Micro Electro Mechanical Actuators”, 22nd International Conference on Microelectronics (MIEL 2000), Nis, Serbia.
27. Tanner, D. (2009), “MEMS Reliability: Where Are We Now?”, Journal of Microelectron Reliability, Vol. 49, 3, pp. 937–940.
28. Totaro, M., Bruschi, P. and Pennelli, G. (2012), “Top down Fabricated Silicon Nanowire Networks for Thermoelectric Applications”, Journal of Micro electron Engineering, Vol. 97, 2, pp. 157–161
29. Tripp, M., Stampfer, C., Miller, D., Helbling, T., Herrmann, C.and Hierold, C. (2006), “The Mechanical Properties of Atomic Layer Deposited Alumina for Use in Micro- And Nano-Electromechanical Systems”, International Journal of Sensors Actuators, Vol. 130, 1, pp. 419–429.
30. Rebeiz, M. G. (2003), “RF MEMS Theory, Design and Technology”, Wiley Publications, Canada.
31. Spengen, W. (2003), “MEMS Reliability from a Failure Mechanisms Perspective”, International Journal of Microelectronic Reliability, Vol. 43, 2, pp. 1049–1060.
32. Vardhan, V. K. (2003), “RF MEMS and Applications”, John Wiley and Sons Ltd., England.
33. Wei, G., Shouwen, Y. and Ganyun, H. (2006), “Finite Element Characterization of Size-Dependent Mechanical in Nano Systems”, International Journal of Nano Technology, Vol. 17, 2, pp. 1118–1122.
34. Yang, C., Cheng, Y.and Hsu, W. (2010), “The Investigation of Nano Roughening Effect on the Reliability Enhancement of Adhesive Bond for Manufacture Application”, Journal of IEEE Trans Adv. Package, Vol. 33, 3, pp. 356–361.

35. Yapu, Z. (2003), “Stiction and Anti-Stiction in MEMS and NEMS’, Journal of Acta Mech Sinica (English Series), Vol. 19, 3, pp. 1–10
36. Yoon, S., Yazdi, N., Perkins, N. and Najafi, K. (2006), “Micro Machined Integrated Shock Protection For MEMS”, International Journal of Sensors Actuators, Vol. 130: pp. 166–175.
37. Zaghloul, U., Papaioannou, G., Bhushan, B., Coccetti, F., Pons, P. and Plana, R. (2011), “On the Reliability of Electrostatic /MEMS Devices: Review of Present Knowledge on the Dielectric Charging and Stiction Failure Mechanisms and Novel Characterization Methodologies”, International Journal of Micro electron Reliability, Vol. 51, 1, pp. 1810–1818.
38. Zhao, Y., Wang, L. and Yu, T. (2003), “Mechanics of Adhesion in MEMS—A Review”, Journal of Adhesion Sci. Technology, Vol. 17, 2, pp. 519–546.
39. Zhu, Yong, E. and Horacio, D. (2004), “Reliability of Capacitive RF MEMS Switches at High And Low Temperatures”, International Journal of RF and Microwave Computer-Aided Engineering, Vol.-14, 4, pp.-317-328.
40. Zou, M., Cai, L., Wang, H., Yang, D. and Wyro, T. (2005), “Adhesion and Friction Studies of a Selectively Micro/Nano-Textured Surface Produced By UV Assisted Crystallization of Amorphous Silicon”, Tribology Letters, Vol. 20, 1, pp. 43–52.